FOREWORD

This report was prepared for the United States Air Force by the Cornell Aeronautical Laboratory, Inc., Buffalo, New York, in partial fulfillment of Contract AF33(616)-7517.

The work reported herein was performed by the Flight Research Department of the Cornell Aeronautical Laboratory under sponsorship of the Flight Control Laboratory,* Aeronautical Systems Division, Air Force Systems Command, Wright-Patterson Air Force Base, Dayton, Ohio as Project No. 8219, Task 821905. ASD project engineers have been R. J. Wasicko and A. G. Jones of the Flight Control Laboratory.

Significant contributions to the engineering effort of this project were made by the following Cornell Aeronautical Laboratory personnel: R. Rice, W. Close, C. Matheis, J. Beilman, A. Schelhorn, R. Harper, W. Wilcox, N. Infanti, and W. Breuhaus.

The report is also published as Cornell Aeronautical Laboratory Report No. TE-1462-F-3.

*Now designated AF Flight Dynamics Laboratory

ABSTRACT

The criteria, design, installation and flight calibration of a variable drag system are discussed. The system allows for variable L/D characteristics in the variable stability T-33 airplane.

With this system in the special T-33, the airplane will be used to investigate the interactions between handling qualities and many drag characteristics including very low L/D and shapes of L/D curve for high L/D ratios.

PUBLICATION REVIEW

This report has been reviewed and is approved.

FOR THE COMMANDER:

C. B. Westbrook

C. B. WESTBROOK
Chief, Control Criteria Branch
Flight Control Division
AF Flight Dynamics Laboratory

TABLE OF CONTENTS

LIST OF ILLUSTRATIONS

LIST OF ILLUSTRATIONS
(continued)

LIST OF TABLES

LIST OF SYMBOLS

a_x	longitudinal acceleration, g's
C_D	coefficient of drag
C_{De}	coefficient of effective drag
C_{D_F}	coefficient of drag due to flaps
C_{D_α}	coefficient of drag variation with respect to angle of attack
C_L	coefficient of lift
C_T	coefficient of thrust
D	drag
D_e	effective drag
D_P	drag due to petals
g	gravitational constant (32.2 ft/sec^2)
G.W.	gross weight, pounds
h_p	pressure altitude, feet
K_C	cockpit gain control, δ_p/α
K_D	cockpit gain control, δ_p/V_e
K_E	cockpit trim control, $\delta_{p_{TRIM}}$
L	lift
m	mass of airplane, slugs
$\bar{q}$	dynamic pressure, $1/2\,\rho V^2$
S	wing area, feet^2
T	thrust of airplane, pounds
V	velocity, knots
V_e	equivalent velocity, $V\sqrt{\sigma}$
V_{IAS}	indicated airspeed, knots
W	weight, pounds

X_u	X force due to speed change
X_α	X force due to angle of attack
α	angle of attack, deg
γ	flight path angle, deg
δ_e	elevator displacement, deg
δ_F	wing flap position, deg
δ_{LG}	landing gear position, deg
δ_p	L/D petal position, deg
Θ	pitch angle, deg
ξ	angle between the thrust vector and the x-body axis
τ	time constant

INTRODUCTION

Aircraft with highly-swept wings, aircraft with delta wings, and re-entry glide vehicles all have the problem of low aerodynamic L/D values. For these types of aircraft, the maximum lift-to-drag ratio occurs well above touchdown speed, and usually above final approach speed. Thus, pilots are forced to fly final approaches on the "back-side" of the lift-to-drag ratio curve if they are to have low approach speeds and this, together with the low lift-to-drag ratio, complicates the task of precisely controlling the steep final approach path. Flight on the back side of the L/D curve makes it quite difficult for the pilot to choose the proper flare-point to obtain low sink rates at touchdown. If the pilot increases airplane angle of attack, the flight path becomes steeper. This is in direct contrast to flight on the front side of the L/D curve, where increasing the angle of attack results in a shallower flight path.

In vehicles that have engines, drag can be offset by changing engine thrust and the effective lift-drag ratio, and consequently the cotangent of the flight path angles is held close to 15 on the final VFR approach and higher than this for any type of IFR approach.

A re-entry vehicle will be without engine thrust for most, if not for all, of the landing approach. If a re-entry vehicle has an engine to allow a single "go-around", in the event of an aborted landing, then the pilot may use the thrust on either the first or the second approach to help adjust the landing-approach path. It is also possible that re-entry vehicles will not have "go-around" engines, and their pilots will have to rely entirely on their skill to establish and hold a proper glide path. The effective L/D for an engineless re-entry vehicle is probably never greater than 4. This characteristic implies that the landing-approach glide angle will never be less than fourteen degrees, and that any adjustment of the glide angle will strongly affect the remaining available range of the glide vehicles.

To assure successful missions in low L/D vehicles it is important to determine the effects of low L/D in the presence of various combinations of both longitudinal and lateral-directional handling qualities in order to determine handling characteristics interaction phenomena. An airplane in which both the longitudinal and lateral-directional handling characteristics can be separately varied is the variable stability T-33, which is operated by the Cornell Aeronautical Laboratory for the United States Air Force. To use this airplane for investigating the interaction of handling qualities with flight path characteristics, a variable L/D system was designed for installation in the special T-33. This report describes the system selected, and discusses the criteria used for the design of the system.

The report is divided into several sections which are outlined below.

Original manuscript submitted October 1962; revised manuscript released by the author August 1963 for publication as an ASD Technical Documentary Report.

FIGURE 1 DRAG PETALS, WITHOUT PETAL EXTENSIONS, ON T-33 TIP TANKS

SECTION 1

THE VARIABLE L/D SYSTEM

The initial problem in designing the variable L/D system was to determine the particular drag augmentation system to use. Modulated thrust reversers, spoilers and drag petals were investigated. The criteria for choosing among the systems are:

a. The amount of drag produced for a minimum interference with airplane stability and aerodynamic control effectiveness,
b. Minimum trim change, and
c. Practical instrumentation-control-system design requirements.

Both the target type and the cascade type thrust reversers, in the region of maximum effectiveness produce large trim changes and require very stringent precision control. These characteristics were determined from References 1, 2, and 3.

The characteristics of spoilers were determined from References 4, 5, 6, and 7 and sets of spoilers were designed and fabricated for testing on a 1/10 scale wind tunnel model. The predicted characteristics for the spoilers were discouraging.

A third technique, drag petals mounted on the airplane-wing tip tanks, was investigated and 1/10 scale petals were fabricated for use on the wind tunnel model.

The wind tunnel tests of the spoilers and the drag petals corroborated the predictions for the spoilers but not the predictions for the petals. That is, the spoilers would be large, they would affect airplane stability and trim and they would compromise aileron effectiveness. On the other hand, the petals produced considerably more drag than predictions indicated they would and they did not affect airplane stability or trim, nor did they compromise aileron effectiveness.

After a review of the thrust reverser data and the wind tunnel data for both many spoiler configurations and the petals, the decision was to develop the petal system for installation on the special T-33.

Spoiler and drag petal characteristics are given in Reference 8, the wind tunnel report. Important aerodynamic characteristics of the drag petals are included and are discussed as the design of the drag system is developed.

Reference to effective L/D or $(L/D)_e$ is often made in the report. This value of L/D is different from the aerodynamic L/D in that the former accounts for the amount of drag that is cancelled by residual thrust from the "idling" jet engine of the T-33. At sea level this thrust is approximately 600 pounds at an engine rpm somewhere between 50% and 60% of normal rated rpm. At 10,000 feet altitude, the residual thrust is approximately 300 pounds. The steady-state-flight definition of $(L/D)_e$ is given in Figure 2.

The design of the drag petal system is divided into the following areas:

aerodynamic, mechanical, hydraulic, electronic and safety of flight. Both the design criteria and the safety of flight criteria are common to all areas, and a general understanding of the system is most easily developed by considering these criteria first.

A. CRITERIA FOR PETAL SIZE

The system must develop sufficient drag that an effective L/D of four and less can be obtained with the T-33 at the landing-approach speeds of swept wing, delta wing and re-entry aircraft. This speed is generally greater than 140 knots. At 140 knots the T-33 landing gear, wing flaps and dive brakes can all be fully extended. For the "dirty" T-33 at 140 knots, the basic L/D = C_L/C_D is 5.3. The effective L/D is 7.1, assuming 600 pounds of engine thrust, for a 12,000 pound T-33. An engine thrust of 600 lb will occur at low altitudes for an engine speed somewhere between 50% and 60% normal rated rpm. The 12,000 lb weight assumed is the probable mean weight of the airplane while evaluation flights with the variable L/D system are made. These characteristics are shown in Figures 3 and 4. Figure 4 also shows the C_L vs. C_{D_e} that is required for an $(L/D)_e = 4$. From Figure 4, by comparing C_L vs. C_{D_e} for the airplane to that required for $(L/D)_e = 4$, it is seen that, at 138 knots for a 12,000 pound "dirty" T-33, $\Delta C_D = 0.09$ is required. If only the dive brakes were extended, then a ΔC_{D_e} of 0.12 would be required. The value of $\Delta C_{D_e} = 0.12$ is very nearly the maximum value of ΔC_D that the tested petals produced, as shown in Figure 5. Hence, by scaling up the area of the tested petals it is found that each full-scale petal should have an area of 7 square feet Furthermore, the wind tunnel tests proved that the effectiveness of the petals depended greatly on transverse extensions at the edges of the petals. The aerodynamic design requirement for each petal is that the petals have 7 square feet of area and that this area include transverse extensions. The general shape of the petal is shown in Figure 6. In this figure the transverse extensions are labeled "petal flanges". For practical purposes, each petal is divided into two parts; the main petal, and the petal extension.

The size of the petal angle is dependent on the angle which the petal makes with the relative wind. In the wind tunnel tests, this angle was a maximum of 90°. However, Figure 5 indicates that a petal angle of 75° or more would be sufficient if the petal area is 7 square feet. The actual angle that is available in the fabricated equipment is 82.5°.

No pressure surveys of the surface of the petals were made during the wind tunnel tests, and the pressure distribution on the petal is assumed to be as shown in Figure 7. If 1000 pounds is the maximum operating load to which each petal could be subjected, then with four petals fully open the obtainable $(L/D)_e$ would be less than 3 for all speeds greater than 140 knots IAS. The 1000 pounds of force per petal occurs at approximately 200 knots IAS for the 7-square-foot petals, and the effective L/D is between 2.5 and 3. The maximum load per petal is specified as 1000 pounds because this load is both reasonable and conservative.

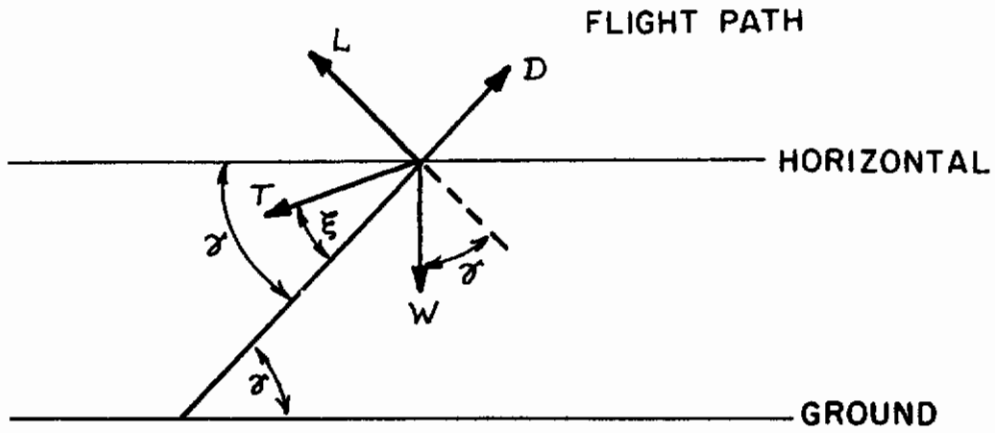

Σ FORCES IN FLIGHT PATH AXES

$L - W\cos\gamma + T\sin\xi = 0$

$D - T\cos\xi - W\sin\gamma = 0$

$D - T\cos\xi \equiv D_e$

$L + T\sin\xi = W\cos\gamma$

$D_e = W\sin\gamma$

$$\frac{L + T\sin\xi}{D_e} = \frac{\cos\gamma}{\sin\gamma} = \cot\gamma$$

$L = qSC_L$

$D = qSC_D$

$D_e = qS(C_D - C_T) = qSC_{D_e}$

$qSC_L = W\cos\gamma$

$qSC_{D_e} = W\sin\gamma$

$$\frac{C_L}{C_{D_e}} = \cot\gamma \neq \frac{C_L}{C_D}$$

unless $T = C_T = 0$

for ξ small (within 1° for T-33):

$$\frac{L}{D_e} = \frac{C_L}{C_{D_e}} \equiv \text{effective } \frac{L}{D} = \left(\frac{L}{D}\right)_e$$

$$\frac{C_L}{C_D} = \text{aerodynamic } \frac{L}{D}$$

FIGURE 2 EXPLANATION OF EFFECTIVE L/D

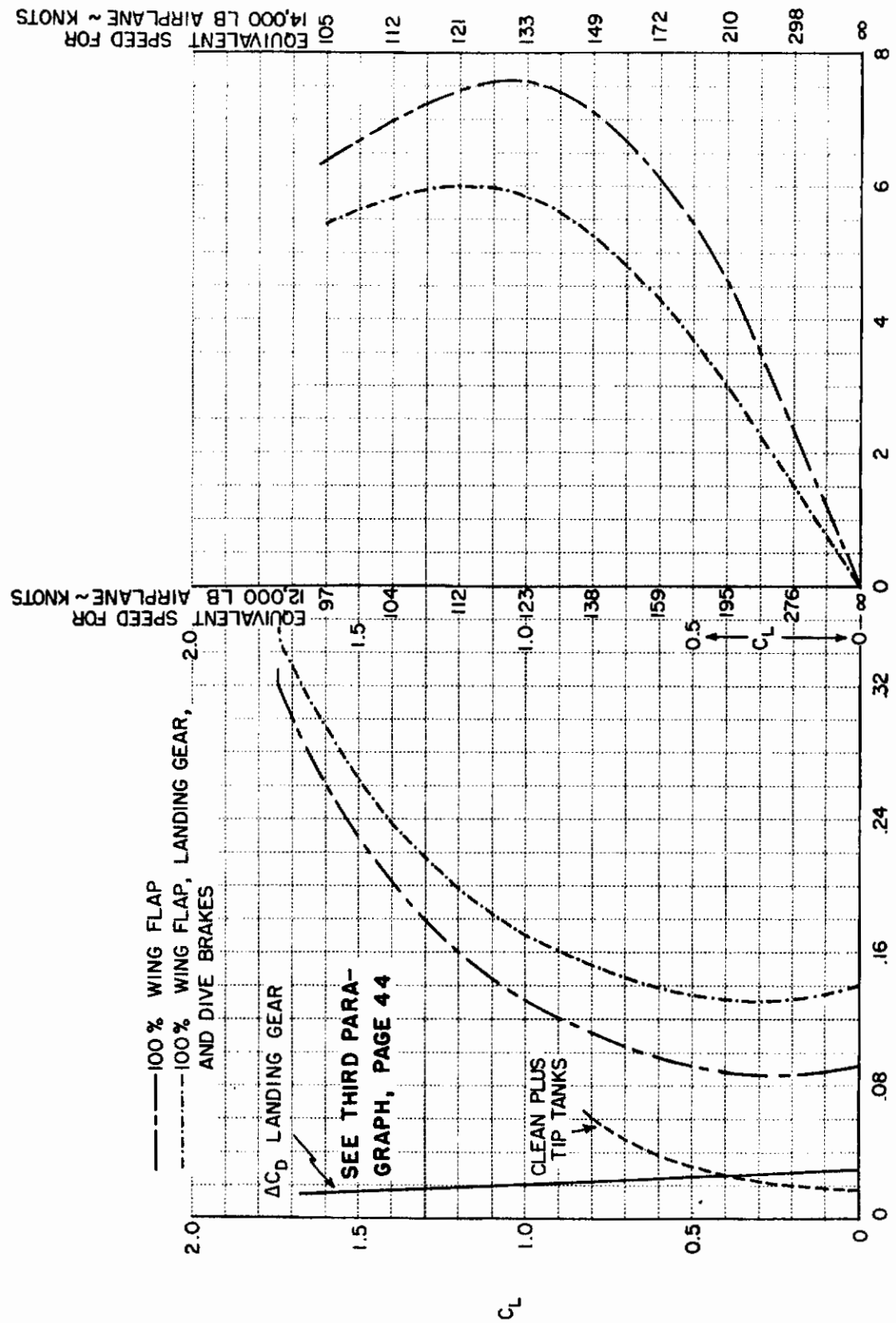

FIGURE 3 AERODYNAMIC LIFT-DRAG CHARACTERISTICS OF T-33 WITH TIP TANKS

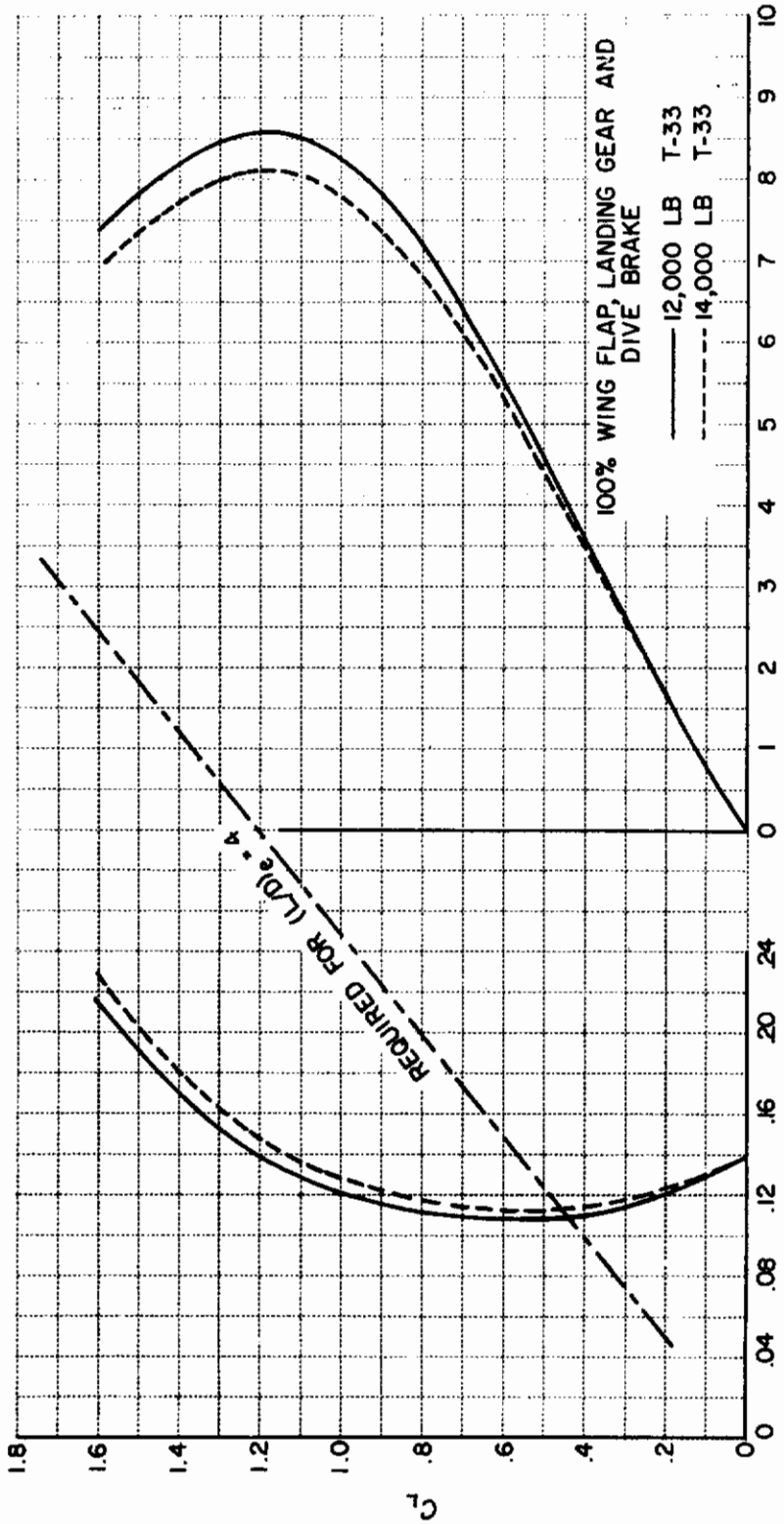

FIGURE 4 EFFECTIVE LIFT-DRAG CHARACTERISTICS WITH MINIMUM SEA LEVEL THRUST OF 600 POUNDS AND TIP TANKS

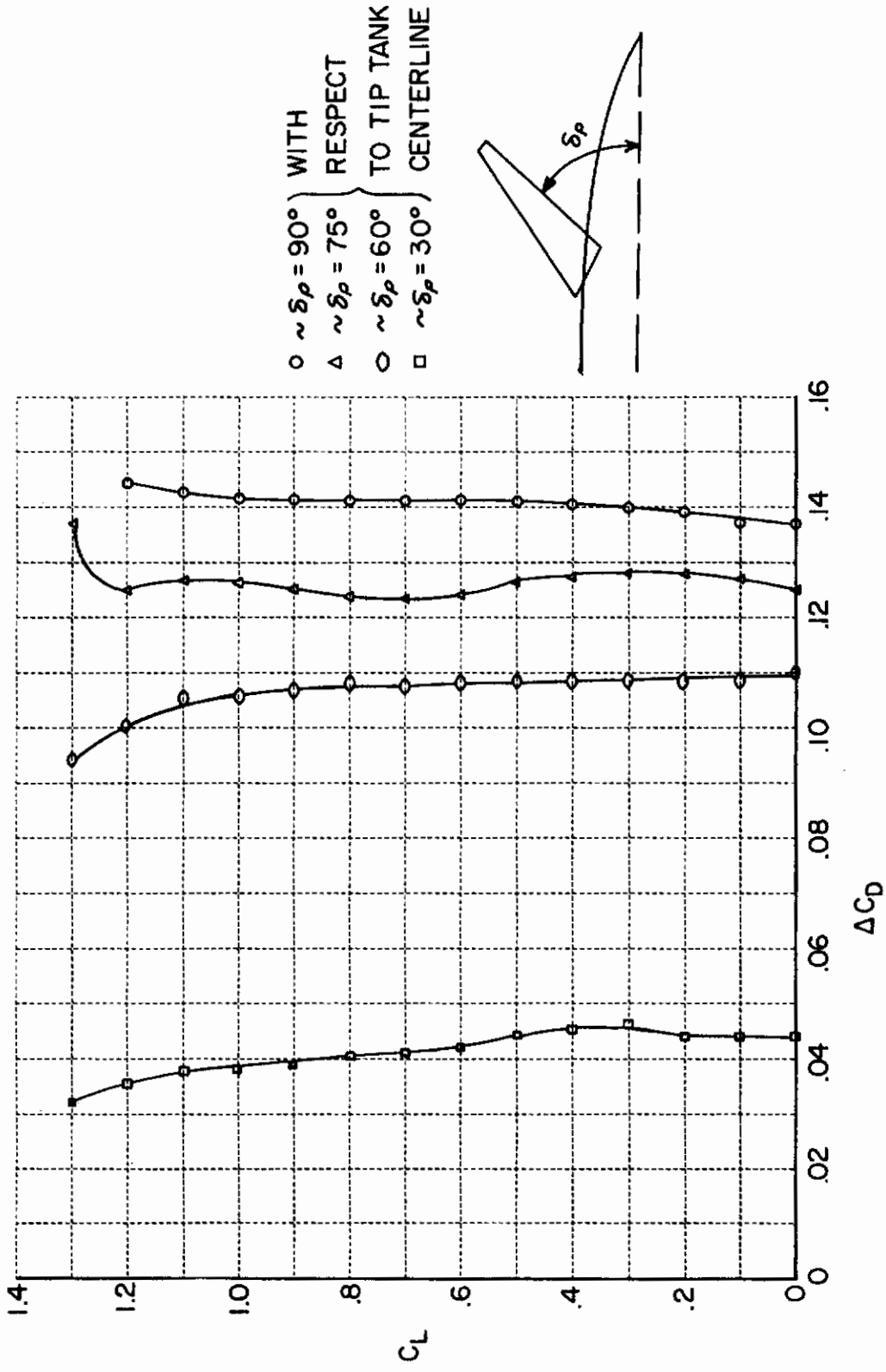

FIGURE 5 C_L VS. ΔC_D FOR DIFFERENT PETAL DEFLECTIONS (WIND-TUNNEL DATA FOR FOUR PETALS)

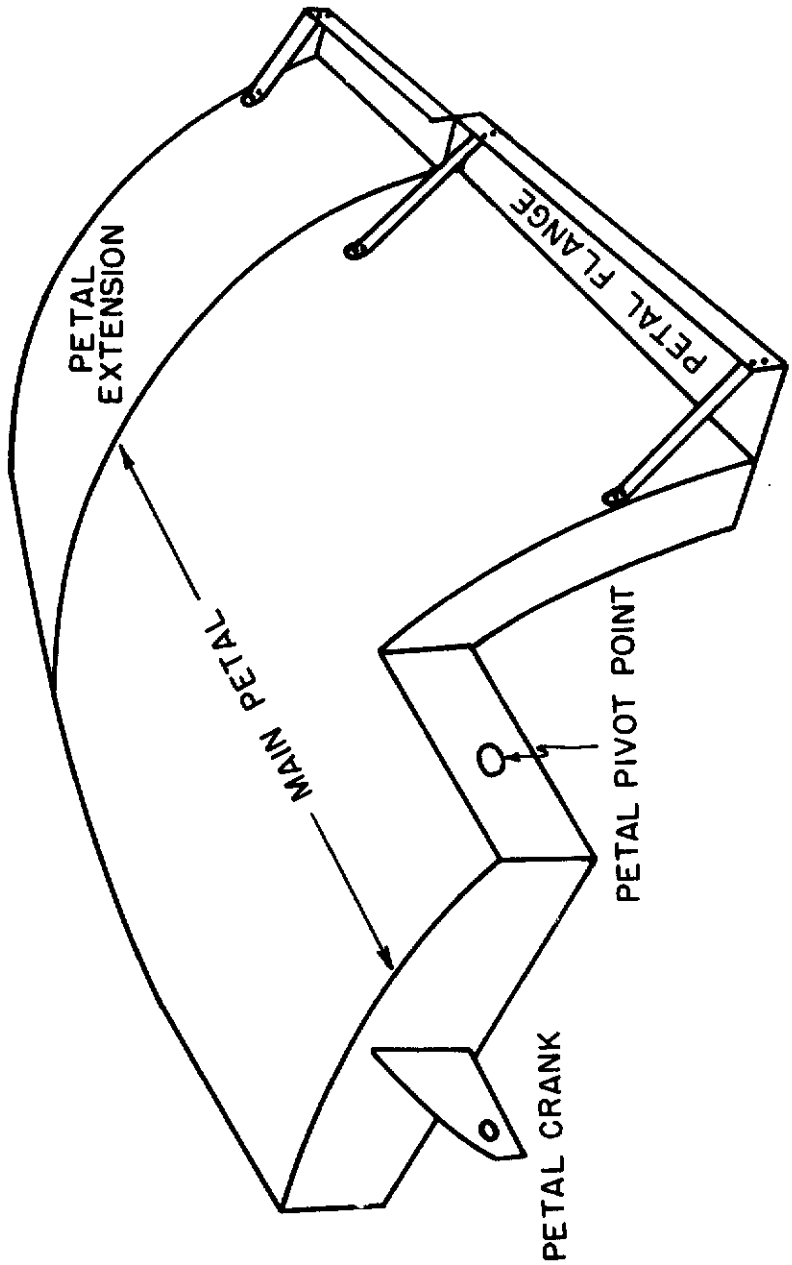

FIGURE 6 PETAL STRUCTURAL SCHEMATIC

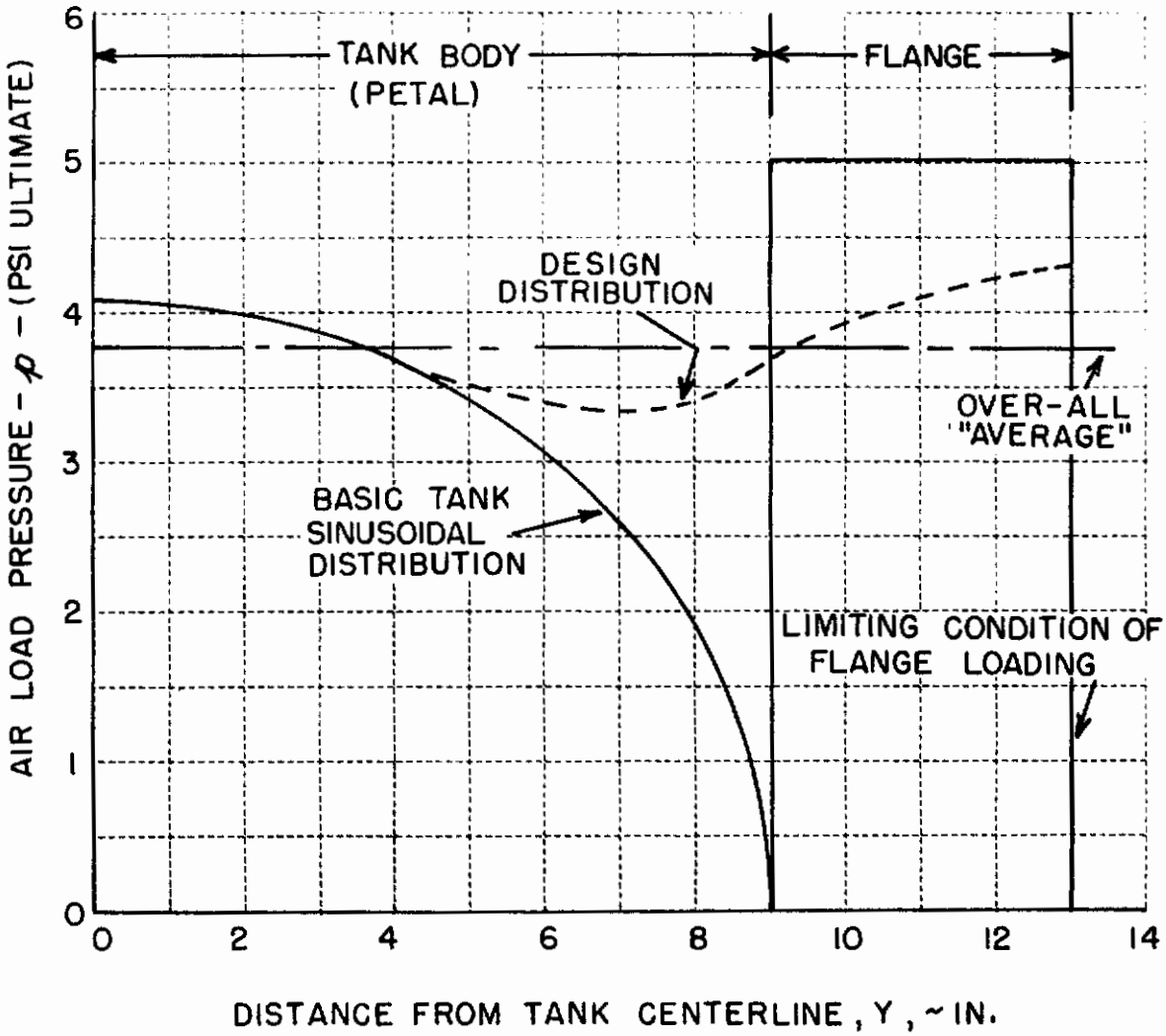

FIGURE 7 AIRLOAD PRESSURE DISTRIBUTION VS DISTANCE FROM TANK CENTERLINE

(PETALS FULL OPEN)

(ADDITIONAL SAFETY FACTOR OF 2 IS INCLUDED IN NUMBERS)

The ultimate design load factor is taken as 1.725. This factor is the limit load factor (1.15) multiplied by 1.50. With two petals per wing tip, the maximum operating load per wing tip is 2000 pounds and the ultimate load per wing tip is 2000 x 1.725 = 3450 pounds. Information supplied by Lockheed indicates that the T-33 wing can withstand more than 3500 pounds of drag force per wing tip.

A second wind tunnel test was performed to assess the flutter boundary of the T-33 wing with the petals installed on the wing-tip fuel tanks. The estimated flutter boundary is considerably above 300 knots IAS and the flutter is a constant dynamic pressure phenomenon.

The following petal design criteria are reasonable in terms of structural integrity of the airplane, flutter characteristics, and general safety of flight considerations. The criteria also mean that the contract requirement of an $(L/D)_e$ of 4 and less is met and that the possible $(L/D)_e$ will likely be 3 and less at speeds greater than 140 knots. The petal design criteria are specified as follows:

1. Number of petals: 4
2. Area per petal: 7 square feet
3. Each petal must have flanges that represent at least 1/5 of the total projected flat plate area of the petal.
4. Except for the flanges the petal will have the same shape as the afterbody of the wing-tip tank
5. Maximum operating load per petal: 1000 pounds
6. Design limit load per petal: 1150 pounds
7. Design ultimate load per petal: 1725 pounds.

The construction and installation of the petals are shown in Figures 8, 9, 10 and 11.

B. MECHANICAL DESIGN CRITERIA

The criteria for the mechanical design of the L/D system are developed from the aerodynamic, hydraulic and safety of flight considerations.

The aerodynamic considerations, which were not listed as petal criteria, are that the petal angle must be continuously variable from zero degrees to at least 75 degrees, that the petal pivot-point should be at a tip-tank station that is nearly coincident with the intersection of the tank and the wing trailing edge, and that the petals should not interfere with the ailerons or require any revision of the ailerons to be made. The specification of the approximate pivot point is a result of the desire to duplicate the pivot point of the petals that were used in the wind tunnel tests and, furthermore, the area and shape specifications of the petal dictate that the pivot point must be positioned approximately as specified. Such a position of the pivot point does not result in any mechanical interference between the petals and the ailerons, and the aerodynamic interference will be small and in accordance with the wind tunnel data that is shown in Figure 12.

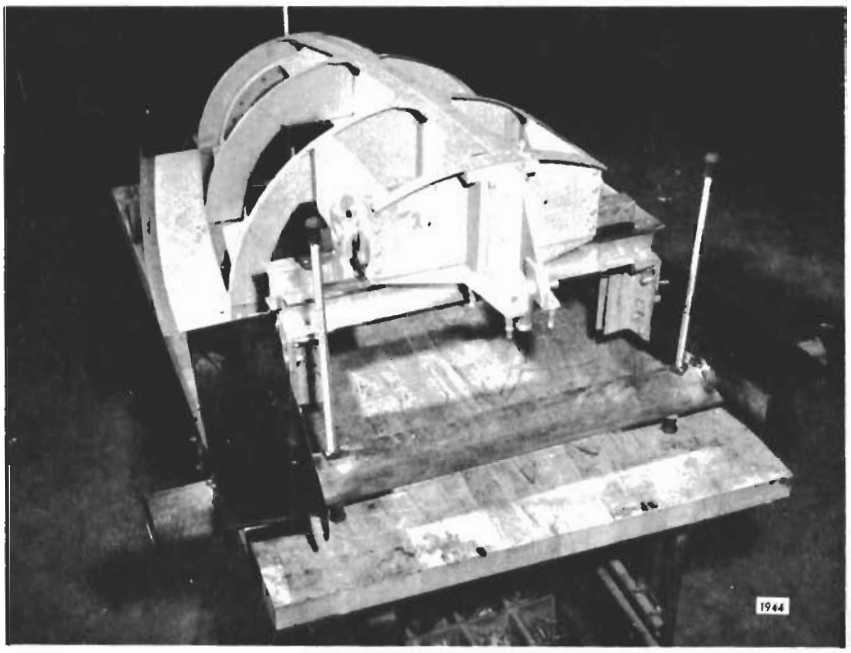

FIGURE 8 MAIN PETAL CONSTRUCTION: BASIC FRAMEWORK

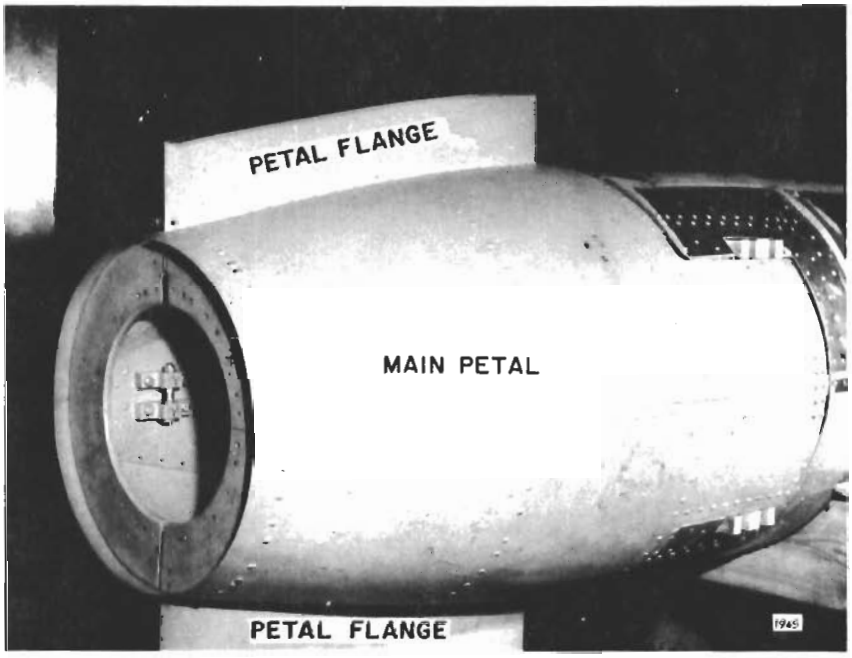

FIGURE 9 MAIN PETAL CONSTRUCTION: CLOSED POSITION

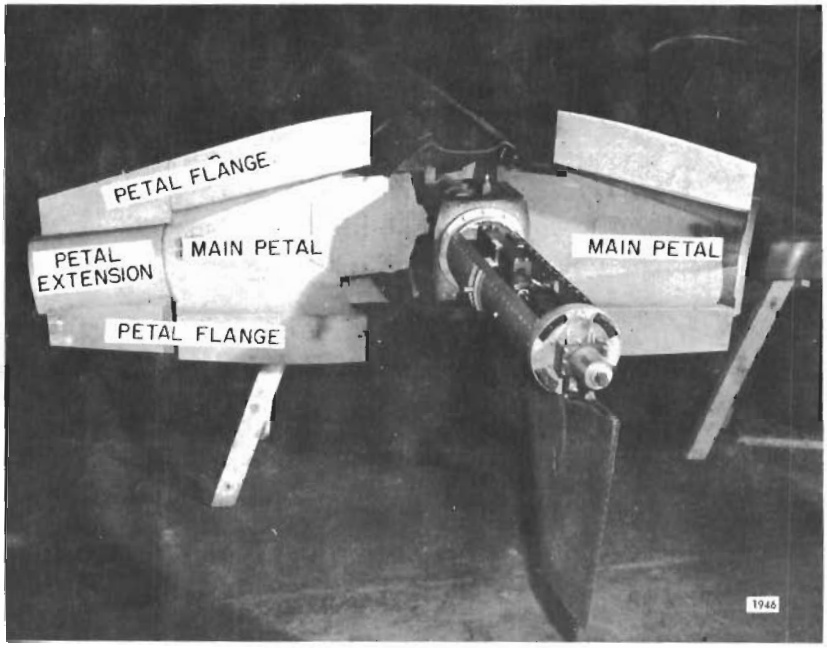

FIGURE 10 PETAL CONSTRUCTION: FULL-OPEN POSITION

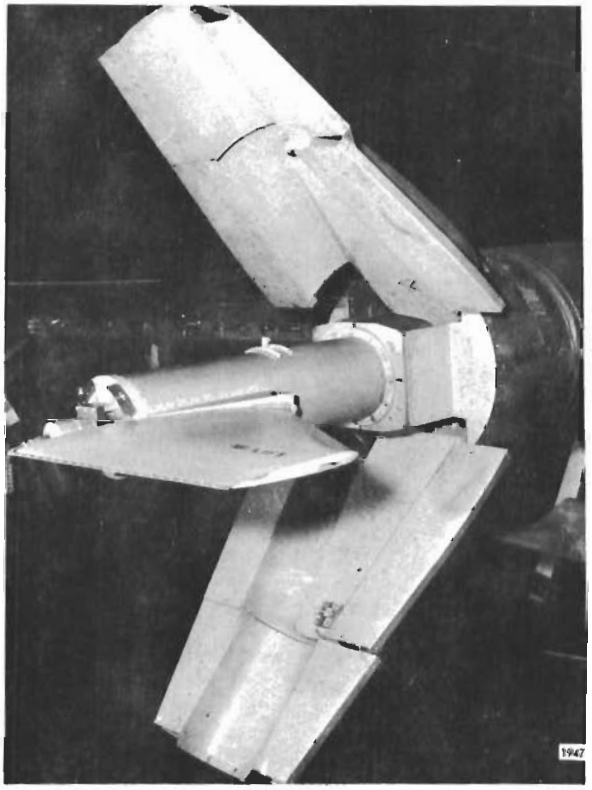

FIGURE 11 PETALS IN HALF-OPEN POSITION

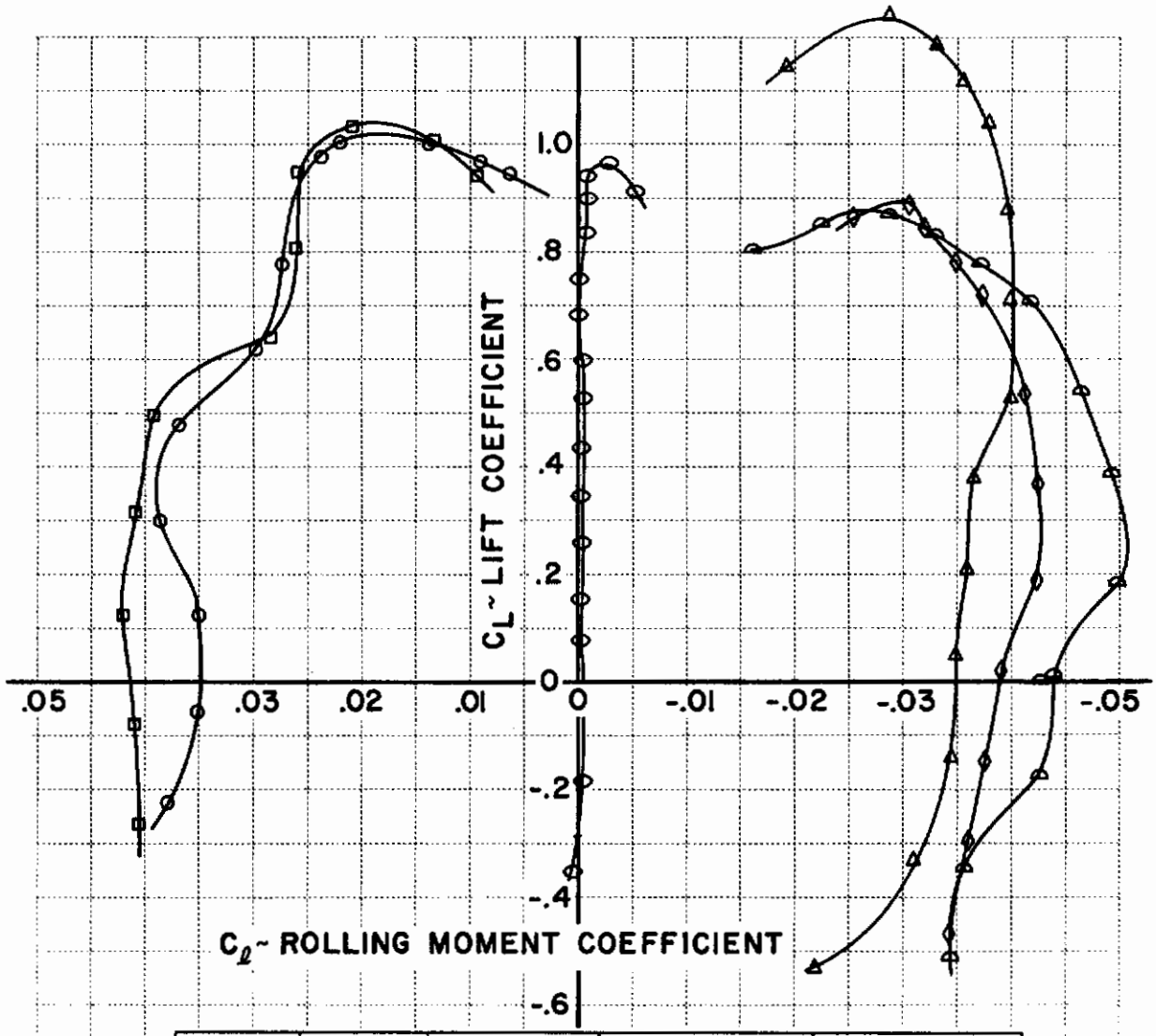

SYMBOL	TAIL ON	FLAP DEFL. DEG	LEFT AILERON DEFL. DEG	PETALS
△	✓	45	20° T.E. UP	ALL 4 AT 90°
⬭	✓	0	0	"
◇	✓	0	20°	"
○	✓	0	-20° T.E. DOWN	"
□	✓	0	-20°	CLOSED
⌓	✓	0	20°	"

FIGURE 12 AILERON POWER - LEFT AILERON ONLY FOR PETALS FULL OPEN AND CLOSED

Hydraulic system considerations that are pertinent to the mechanical design are also safety of flight considerations. The tip tanks must remain jettisonable, and therefore any hydraulic lines between the airplane and the tip tanks must be arranged to separate easily, quickly, and not interfere with the jettison action.

Petal actuation is so arranged that, when the petals are not being commanded, they will be blown shut and held in the closed position by a latch. The latch is so made that it will not lock whenever the petals are being commanded. Such a requirement is necessary to insure that a latch will not capture a petal in the closed position during normal command operation of the petals.

The tip tank fin that is required for tank stabilization during jettison is retained.

The normal tip tank can withstand a drag load of 7907 pounds (ultimate). Therefore, no analysis of the tank load-carrying ability is necessary.

Each standard tank can carry 230 U. S. gallons of fuel. It was desired to retain as much of this capacity as possible to keep the useful test time per flight at a maximum.

According to the wind tunnel flutter tests, the flutter speed is sufficiently high with the petal actuation mechanism mounted in the rear of the tip tank that it is unnecessary to consider mounting any part of the L/D system in the forward part of the tip tank to adjust both the tip tank c. g. position and the flutter speed.

To summarize the mechanical design criteria:

1. The petal angle must be continuously variable from zero degrees to at least 75 degrees.
2. The pivot point of the petals will be at a tip tank station near the intersection of the wing trailing edge and the tip tank.
3. The tip tanks must remain jettisonable.
4. The tip tank fin must be retained.
5. Low-force quick disconnects must be arranged for all electrical and hydraulic connections between each tip tank and the airplane.
6. Whenever the petal actuation system is not pressurized the petals must be free to be blown closed.
7. Latches must be provided to hold each petal closed whenever the petal actuation system is not pressurized, but the latches will be inoperative whenever the petals are being commanded.
8. As much of the fuel capacity of the tip tanks as possible must be retained.

C. CRITERIA FOR HYDRAULIC SYSTEM

The hydraulic system design criteria were developed after investigating several methods for obtaining the prime power for the petal actuation

system. Some of the methods are: engine bleed air; externally mounted auxiliary power units; electrically driven power units; an engine-driven hydraulic pump. Sufficient power to drive the petals could not be obtained from either the available electrical power or bleed air power. A considerable amount of information on a through-shaft hydraulic pump was available, and therefore, design criteria of the hydraulic system were based upon the use of this system.

To determine the horsepower requirements for the petal actuation system, a petal duty cycle was first determined. The duty cycle is predicated to have the petals follow angle of attack changes during a typical airplane longitudinal short period response, and assumes that, on a landing approach, the airplane may lose speed at the rate of 3.5 knots per second. At an equivalent airspeed of 140 knots in the T-33, while maintaining an L/D of approximately 3, the resulting maximum petal rate is approximately 30 degrees per second. When the petal rate is converted into the flow rate required at 3000 psi pressure, it is found that 7.8 mechanical horsepower are required from the engine to drive the hydraulic pump. Because the 1000 psi hydraulic pump already in the airplane will be driven in tandem with the through-shaft pump, the mechanical horsepower required by the 1000 psi pump must be added to the 7.8 horsepower required for the through-shaft pump. The total horsepower for both pumps is 10.4, which is 2.4 horsepower greater than the 8 horsepower maximum continuous rating at 2000 rpm for the engine accessory drive pad on which the pumps will be mounted. Therefore, the output flow of the 3000 psi through-shaft pump must be limited to 2.5 gallons per minute at 2000 rpm to keep the horsepower requirements within the limits of the accessory pad. The additional horsepower required for peak petal rates only is supplied by an accumulator. With this arrangement the 3000 psi, through-shaft pump requires 5.3 horsepower and delivers 4.8 flow horsepower, which is the average demand of the L/D system, equivalent to a petal rate of twenty degrees per second. A one-gallon accumulator in which the gas precharge pressure is 2600 psi provides the additional horsepower requirements. Whenever the petals are used to maintain an L/D of four there are no demands on the accumulator until the equivalent airspeed of the T-33 drops below 150 knots, if the wing flaps are down. If the wing flaps are up, then demands on the accumulator occur for equivalent airspeeds less than 170 knots.

An external by-pass for the through-shaft pump is required because the pump has no internal by-pass, and yet to keep the pump from overheating and possibly seizing there must be a continual flow of hydraulic oil through the pump. Because there will be a sufficient flow of oil through the pump whenever the L/D system is engaged, then the by-pass will be required only when the L/D system is not engaged. The physical arrangement of the pumps makes it impossible to declutch the through-shaft pump whenever the L/D system is not engaged.

For safety the hydraulic system must be designed to prevent hydraulic lock of the petals, and to allow the petals to blow back against system pressure if the drag force per petal exceeds 1000 pounds. The blow-back provision must be common to both sets of petals to prevent either from blowing back while the other does not move. Otherwise, through possible malfunction, one set of petals might blow back while the other set remains fixed, resulting in uncontrollable yaw of the airplane.

The blow-shut requirement provides for free movement of the petals whenever the L/D system is not engaged and whenever the petals are not latched shut. This requirement ensures that, if the petals cannot be commanded shut, the system can then be disengaged and the petals will be blown shut.

Because the hydraulic pump requires a positive inlet pressure of at least 5 psi (gauge) to avoid cavitation, the hydraulic reservoir should be pressurized. The reservoir must be separate from any hydraulics already existing in the airplane and a reserve supply of hydraulic oil should be provided for cooling the through-shaft pump in the event that the primary oil supply is lost through a leak or other malfunction. The reservoir should have a capacity of approximately 2 gallons; one gallon for the primary supply and the second gallon in reserve.

To summarize hydraulic design criteria:

1. Use the 3000 psi through-shaft pump and a 1-gallon accumulator with a precharge gas pressure of 2600 psi as the L/D power source.
2. The petals must be able to blow back, against system pressure, whenever the drag force per petal is greater than 1000 pounds.
3. The petals must be free to blow shut whenever they are open and the system is not engaged.
4. Provide a two-gallon reservoir in which one gallon of hydraulic oil is a reserve supply.
5. Provide for pressurization of the hydraulic reservoir.

D. CRITERIA FOR ELECTRONIC SYSTEM

The electronic equipment must be versatile enough to allow for simple, quick changes in function generation. It must include system monitoring circuits that automatically ensure safe flight operation of the L/D system. The equipment must have simple preflight system and calibration check-out techniques.

Among the generated functions which must be simply and easily changed, petal angle vs. equivalent airspeed is important. This is the function by which the $(L/D)_e$ vs. V_e profile is programmed. The profile is programmed as a function of V_e because the range of V_e of interest can be duplicated in the T-33. In contrast, the range of angle of attack of the T-33 will not generally duplicate the range of angle of attack of any swept wing airplane. Nevertheless, it is desirable to have perturbations in drag that follow angle-of-attack perturbations. This is accomplished by programming the desired L/D profile as a function of V_e with T-33 angles of attack. The V_e signal is then used to adjust the gain on the angle-of-attack signal, which from trim conditions transforms the L/D profile as a function of V_e into an L/D profile as a function of T-33 angle of attack. The angle-of-attack signal modified by the gain according to V_e is the primary petal command signal.

Because the maximum test time per filght is little more than an hour, and because a pilot evaluation of a given L/D profile is expected to require approximately one-half hour, there will be provisions for two different

programmed L/D profiles. A cockpit switch must be provided by which either of the profiles can be chosen during a flight.

Fully opened petals will not produce sufficient drag for the low L/D values at low (140 knots) airspeed. Consequently, the wing flaps, landing gear, and dive brakes will be deployed during an L/D evaluation to use their extra drag.

The flaps can be lowered fully at any airspeed below 174 knots. They increase the total drag obtainable, change the pitch trim of the airplane, and alter the zero lift angle of attack by approximately 6°.

It is very likely that the flaps will be lowered at an airspeed greater than the airspeed at which the full drag of the flaps is required. To control the total drag at such a time, the petals must be automatically retracted as a function of flap deflection. This process will keep the total drag constant at the specific airspeed at which the flaps are deployed.

Lowering the flaps creates a pitching moment that puts the airplane out of longitudinal trim. From the closed position, the flaps can be fully lowered in five seconds. This creates a pitching moment requiring the pilot to change the elevator angle by approximately 4° if he is to keep the airplane trimmed. This amount of trim change is very noticeable, and must be automatically compensated as a function of flap deflection. This is easily done by introducing an elevator command signal, which is a function of flap deflection, into the variable stability elevator channel.

The petals will be programmed as a function of V_e, but in order to have a representative C_{D_α} during dynamic maneuvers, the petals must also respond to all changes of angle of attack except for the particular change in angle of attack that occurs by changing the deflection of the flaps. The petals should not follow this change in angle of attack because it is a change between the body axis angle with respect to the wing zero-lift line, and not a maneuvering or perturbation angle of attack. Then, by whatever means the petals are controlled by angle of attack, this means must not be sensitive to changes in angle of attack that are induced by flap-position changes because a change in C_L is not wanted.

Lowering the landing gear also causes a pitch trim change, but does not affect the angle of attack. This pitch trim change is compensated by automatically positioning the elevator as a function of landing gear position.

Because the dive brakes can be used at high speeds, they can always be opened and the airplane can be manually trimmed prior to any L/D evaluation test, and there is no need to consider making automatic corrections for the characteristics of the dive brakes.

The safety features to be incorporated into the electronic instrumentation must complement and aid the safety of flight provisions that are designed into the hydraulic system.

The electronic equipment will monitor the L/D system hydraulic

pressure. If this pressure is less than 2600 psi it will be impossible to engage the L/D system. If pressure drops below 2300 psi during system operation, then the entire system will automatically disengage and leave the petals free to be blown shut. The lower limit of 2300 psi is chosen because the pressure should not fall below this value during a typical duty cycle. If the pressure does fall below 2300 psi, then there is an indication of a malfunction and the system should be shut off.

The petals on one wing tip should track the petals on the other with less than one degree of difference. If the two sets of petals are not tracking each other within one degree, a malfunction is indicated. The practical upper limit of divergence is approximately 10°; beyond this value the task of controlling the airplane in yaw is expected to become difficult as a result of the yawing moment that is produced by the unsymmetrical drag. These estimates are based on wind tunnel data. Therefore, the consistency with which one set of petals tracks the other will be monitored electrically, and if the tracking difference becomes as large as 5° to 10°, then the system will be automatically disengaged. The petals are then free to be blown shut.

The maximum rates at which the petals will ever be expected to move are between 20 degrees per second and 30 degrees per second. Therefore, petal rate will be monitored, and if the rate exceeds some adjustable value, such as 30 degrees per second, then the system will be automatically disengaged. Again the petals will be free to blow shut.

In the event that a break occurs in the petal command-signal loop or the feedback loop, then either the petal differential deflection disengager or the petal rate disengager will disengage the system.

In summary, the L/D electronic equipment design criteria are:

1. Provisions for two programmed L/D vs. V_e profiles per flight; either profile to be chosen at will by the rear seat safety pilot. Each programmed profile will be readily changeable to allow for two new profiles for each successive flight.
2. Automatic compensation for the pitching moments resulting from the position of wing flaps and landing gear.
3. Automatic coordination between petals, flaps and landing gear, so that whenever the flaps and landing gear are lowered, the petals will retract a required amount to keep the total drag at the desired value.
4. The petals must respond to perturbation angle of attack, but must not respond to changes of angle of attack that correspond to changes in the angle of attack for zero lift that result from wing flap extension.
5. For safety of flight, the electronic equipment will be so designed that the L/D system cannot be engaged if the hydraulic pressure is below 2600 psi, and that the system will automatically disengage if, during operation, the hydraulic pressure falls below 2300 psi.

6. To protect against failures of the electronic equipment, the equipment will disengage the system if the petal installations do not track each other within 10 degrees, and if the petal rates exceed a predetermined (but adjustable) value such as 30 degrees per second.
7. If there is a loss of primary power to the L/D electronic equipment, then the system will disengage.

All of the design criteria that are listed have been met. The structural, hydraulic and some of the electronic designs are detailed in Reference 9. The operation and calibration of the L/D system are detailed in the remainder of this report.

SECTION 2
THE HYDRAULIC SYSTEM

The schematic of the hydraulic system is given in Figure 13.

The hydraulic power source is a Kellogg through-shaft, variable displacement pump, type AP6V-S7, mounted directly on the engine accessory pad. The pump supplies a regulated 3000 psi as shown in the calibration of Figure 14. A Vickers relief valve that opens at 3150 psi protects the system from overpressures. The airplane and variable stability system's hydraulic pump (New York Air Brake type 67WS300) is mounted on the back end of the Kellogg pump.

The high pressure hydraulic oil leaves the Kellogg pump, and whenever the system is engaged it passes through an angle-drilling Republic selector valve, a solenoid valve, and out to the L/D servo actuators mounted in each tip tank. The high pressure of the oil is expended in the servo actuator and the oil is returned at low pressure, through a filter, to the hydraulic reservoir. Whenever the L/D system is engaged, the oil supply to the Kellogg pump is from the upper half of the reservoir and is approximately one gallon of oil.

Whenever the L/D system is not engaged, the Republic selector valve returns the pump output to the reservoir, thus providing a system by-pass. Also, with the system in this "by-pass" position the entire capacity (approximately 25 gallons) of the reservoir is in the by-pass hydraulic circuit by virtue of the position of the Parker T-drilling selector valve. The Republic and Parker selector valves are mechanically fastened together and are operated simultaneously through a Teleflex cable connected to a hydraulic selector lever in the rear cockpit.

The hydraulic selector lever can be in either of two positions: "L/D" or "By-pass". If the selector lever is in the "L/D" position and the Tactair solenoid valve (No. 6204-8) is not open at the same time, then the output flow from the pump is blocked. Whenever this situation occurs a red light in each cockpit blinks to warn the pilots of the situation. Upon noting this warning, the rear-seat pilot must immediately take corrective action, because if the pump is blocked for more than a minute or two it will overheat. The pilot can either engage the electronic equipment which will open the Tactair solenoid valve, or he can put the hydraulic selector lever in the "By-pass" position.

As long as the L/D system is engaged, the petals need not be operated to obtain sufficient flow through the pump to keep it lubricated and prevent overheating. The leakage flow through the Moog flow control valves is sufficient to keep the pump lubricated and cool.

Cavitationwill occur in the pump whenever the head pressure at the pump inlet is less than 5 psi (gauge). The required head pressure is obtained by pressurizing the reservoir with pressure that is bled from the engine compressor. At 100% engine rpm the reservoir is pressurized to approximately 20 psi (gauge). If engine rpm falls below 80% the bleed pressure is very low, but a check valve in the reservoir pressure line helps maintain the reservoir pressure at a substantial value.

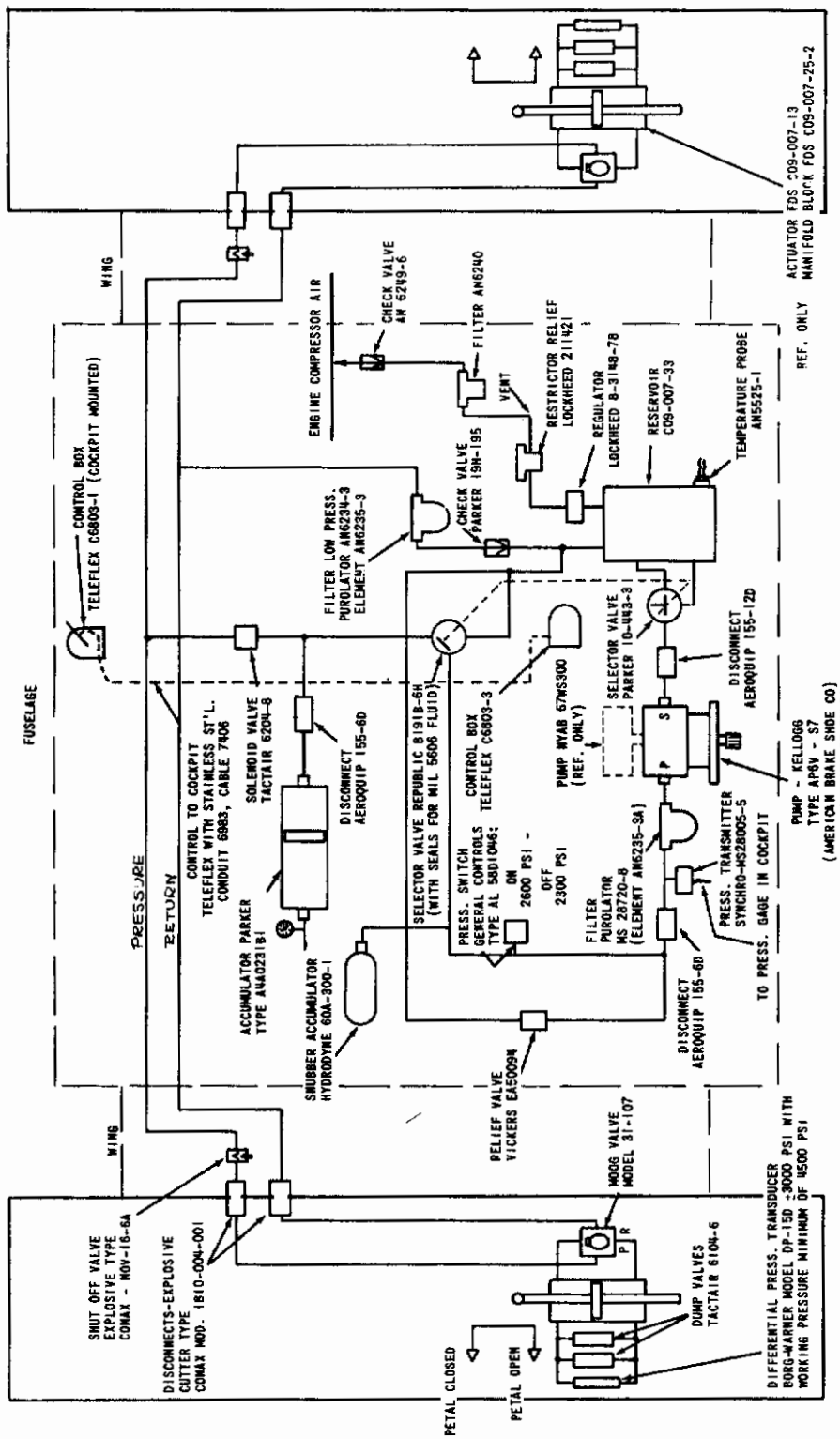

FIGURE 13 SCHEMATIC OF HYDRAULIC SYSTEM

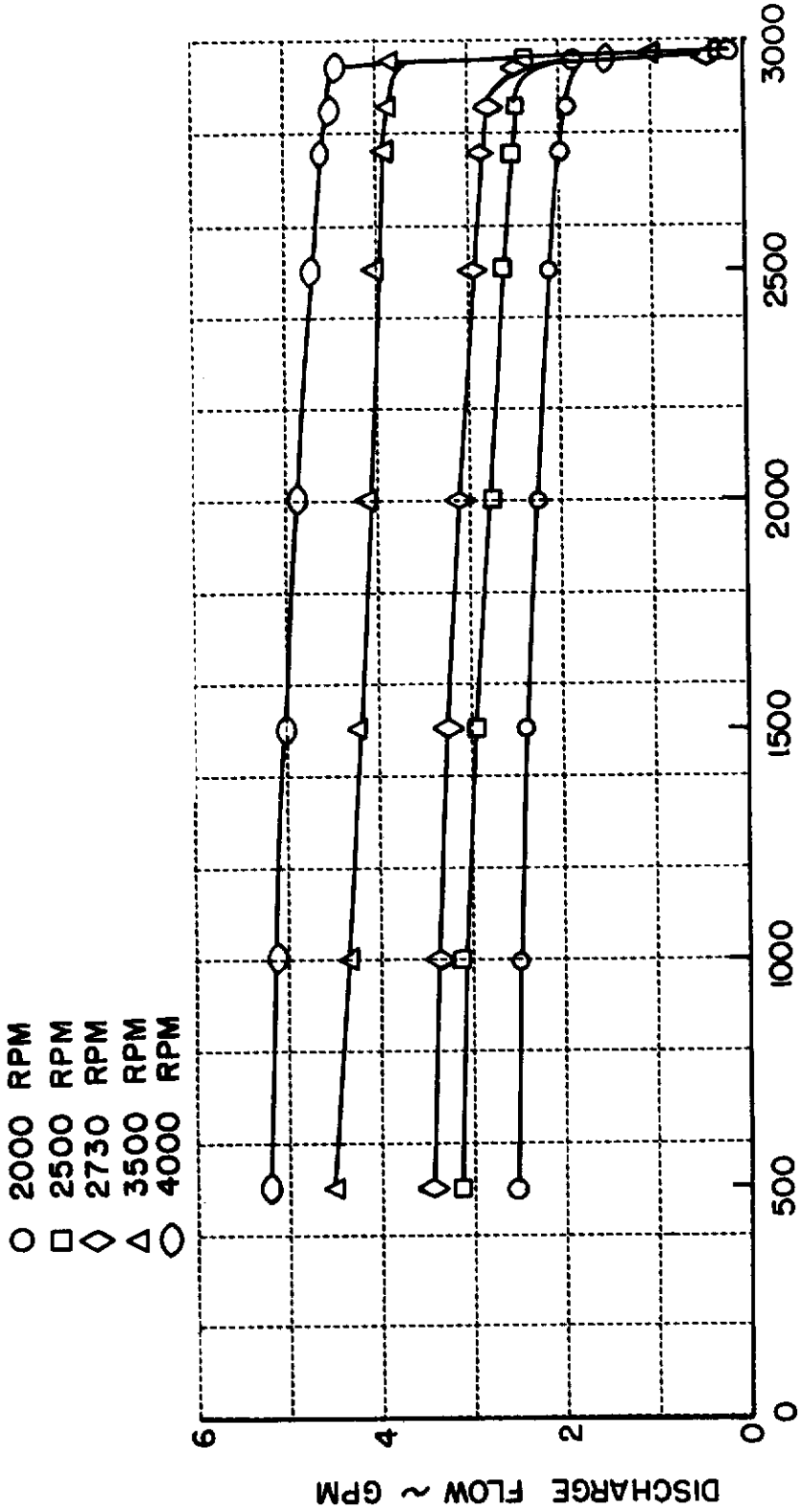

FIGURE 14 KELLOGG PUMP CALIBRATION CURVES

Hydraulic oil temperature and pressure can be read on rear cockpit instruments. Oil temperature is sensed by a thermocouple mounted in the reservoir. Oil pressure is measured, essentially, at the pump outlet. The pressure sensor is protected from valving surge pressures by the Hydrodyne "snubber" accumulator.

Whenever the L/D system is not engaged the Tactair solenoid valve (No. 6204-8) is closed and the Tactair dump valves (No. 6104-6), which are in parallel across each actuator, are open. If the system is engaged, then the solenoid valve is open and the dump valves are closed.

Two dump valves are paralleled to short circuit each actuator upon system disengagement. Such reliability is very necessary. If, when the system was disengaged, one actuator was short circuited but the other was not, due to a malfunction of the dump valve, then one set of petals would blow shut, and the other set would be hydraulically locked open, perhaps wide open. The resulting yawing moment on the airplane might well result in uncontrollability. To ensure against this, two dump valves are paralleled across each actuator.

The last-ditch safety precaution designed into the system allows for jettisoning the tip tanks. The hydraulic lines leading into the tip tanks are continuous 3/8" steel tubing. Each hydraulic line passes through an explosive cutter developed by the Conax Company expressly for this application. To prevent losing hydraulic oil, if a tip tank is jettisoned, each hydraulic pressure line passes through an explosive shut-off valve. Each set of three explosive devices per wing tip is actuated by microswitches which close and fire the devices whenever a tip tank leaves the wing tip by 3/16". This amount of motion cannot occur unless the tank has been jettisoned or has inadvertently become detached from the airplane. The firing sequence of the explosive devices can be chosen by the pilot so that if one tank should fall free then the other tank will automatically be jettisoned and the respective explosive devices will fire. This automatic feature can also be disarmed by the pilot so that if one tank is jettisoned or falls free, then only that tank is lost.

When a tip tank is jettisoned, the L/D system electrical circuits to that tank are disrupted by a pull-apart connector. The electronic equipment senses the disruption and automatically disengages the whole L/D system.

The remaining items of the hydraulic circuit are the General Controls Company pressure switch and the Borg-Warner differential-pressure transducers. The pressure switch makes it impossible to engage the system if the hydraulic pressure is below 2600 psi and automatically disengages the system if pressure falls below 2300 psi.

Pressure feedback is obtained from the differential-pressure transducers and it is used to assure servo system stability above frequencies of 15 cycles per second. This increases the maximum useable frequency response of the system.

SECTION 3

THE INSTRUMENTATION SYSTEM
(A. E. SCHELHORN)

A. GENERAL DESCRIPTION

The electronic instrumentation is a versatile function generator system with inputs from the petals, wing flaps, landing gear, angle of attack, and equivalent airspeed. It is used to control the petals and the elevator according to established functions, particularly any L/D profile that is within the drag capability of the modified airplane. The control system can control the petals as functions of drag versus angle of attack and drag versus equivalent airspeed independently. The system operates the petals and elevator either to compensate drag and trim changes that occur when either the landing gear or the wing flap positions change or to simulate drag and trim changes due to position changes of either landing gear or flaps.

The L/D profile mode and the drag variation with angle of attack and equivalent airspeed are distinct modes of operation. One allows for L/D profile simulation and the other allows for X_α and X_u simulation.

In the L/D profile mode the control signal for the petals is obtained by varying the gain of the angle-of-attack signal as a programmed function of equivalent airspeed.

In the X_α and X_u mode the gains of the angle-of-attack signal and the equivalent airspeed signal are established independently of each other.

The control system provides several safety features for all modes of operation.

L/D Mode

A block diagram of the system providing the L/D profile mode is shown in Figure 15. An angle of attack signal (measured by a vane on the fuselage) is multiplied by (δ_{P_1}/α) to obtain the δ_{P_1} signal. The δ_{P_1}/α function is programmed as a function of V_e (equivalent velocity) and is therefore noted as $[\delta_{P_1}/\alpha]\, f(V_e)$. The function generation technique is explained in detail in Section 3-B. The function is readily changeable to allow programming of desired L/D profiles. Two profiles can be selected in flight.

To maintain low values of L/D at low airspeeds, it becomes necessary to extend the flaps and landing gear. If this were performed manually, the flaps and landing gear would have to be extended at a predetermined airspeed and manual compensation for trim changes made. The drag compensations would have to be programmed into the $[\delta_{P_1}/\alpha]\, f(V_e)$ function and the actuation of the flaps and landing gear would have to be manually synchronized with this function. This cumbersome synchronization task, therefore, has been made an automatic duty of the L/D computer.

Figure 15 shows the method for obtaining the flap and landing gear automatic compensation. The angle-of-attack signal is the measured airplane true angle of attack when the flaps are up. Lowering the flaps changes the fuselage

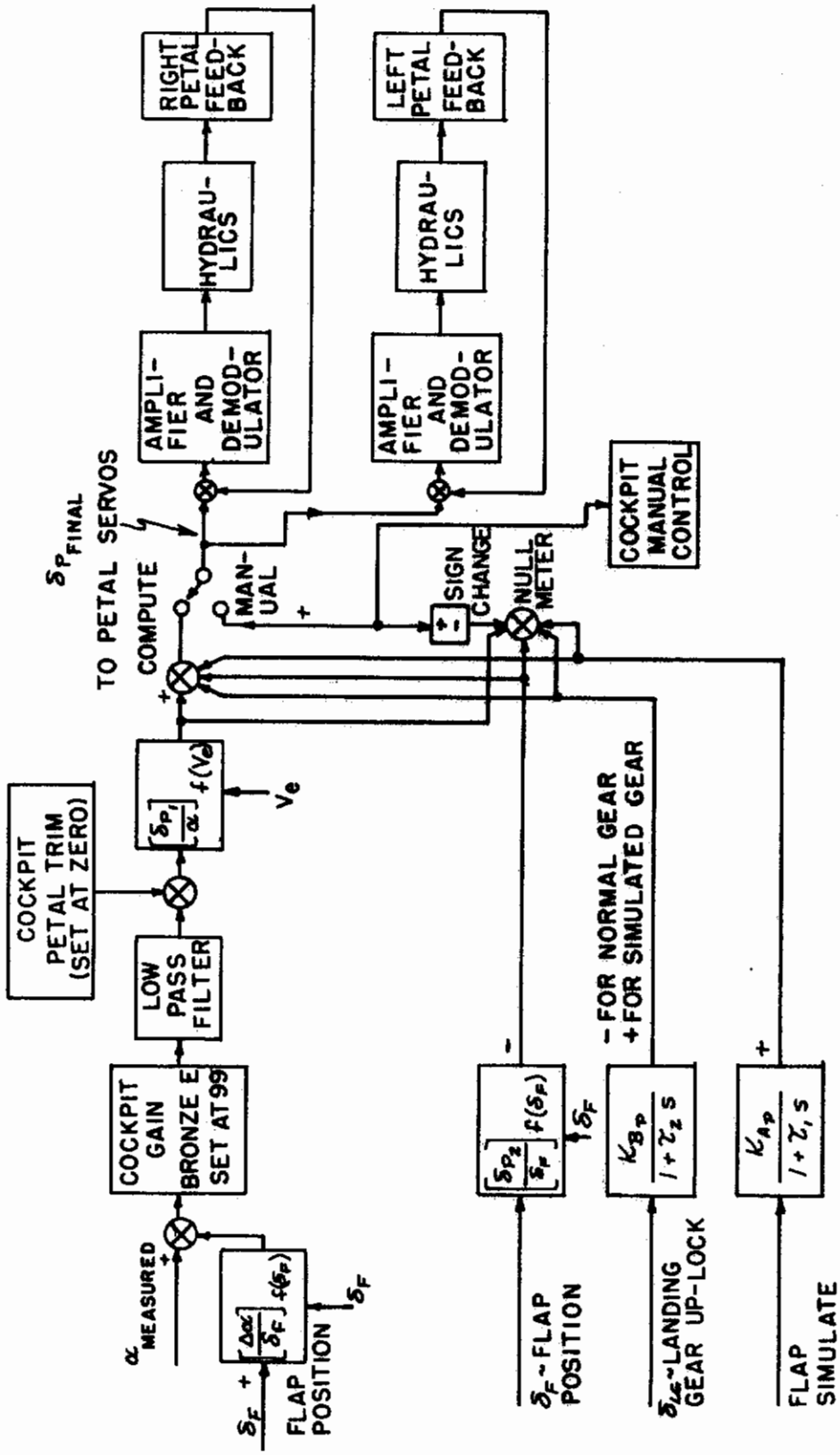

FIGURE 15 L/D PROFILE MODE - BLOCK DIAGRAM

angle of attack required for constant V_e. Therefore, the angle-of-attack signal is modified so that the flap-induced change in angle of attack is removed from the measured angle-of-attack signal. This compensation is accomplished by the function $\left[\Delta\alpha/\delta_F\right]_{f(\delta_F)}$. The angle of attack change due to the landing gear is negligible.

The petal position is modified to compensate for the flap and landing gear drag. Flap position is multiplied by the function $\left[\delta_{P_2}/\delta_F\right]_{f(\delta_F)}$ to provide the correct amount of petal incremental deflection at any flap angle to allow the flap angle to be changed without affecting the total drag on the airplane. Similarly, the landing gear produces a petal angle deflection that gives a drag change which is equal but opposite to the drag of the landing gear. An RC time constant circuit simulates the drag change during the landing gear extension time.

The voltage output of this circuit is summed into the δ_p command signal. The RC circuit is energized whenever the landing gear switch is put in the "landing gear down" position. The settling time of the RC circuit matches the time that the landing gear takes to come down.

The automatic features allow a desired L/D profile to be programmed independently of flap and landing gear positions. If the flap characteristics of a specific vehicle are simulated, the function $\frac{K_{A_p}}{1+\tau_1 s}\,\delta_{F_{SIMULATE}}$ (K_{A_p} and τ_1 are adjustable) would extend the petals to simulate the drag that would result from an actual extension of the flap of the vehicle that is being simulated. The landing gear characteristics of a specific vehicle could be simulated by modification of the $K_{B_p}/1+\tau_2 s\ \delta_{LG}$ function. An equation describing the petal angle deflection during an L/D profile is the following:

$$\delta_{P_{FINAL}} = \left\{\left(\alpha + \left[\frac{\Delta\alpha}{\delta_F}\right]_{f(\delta_F)}\delta_F\right)\left[\frac{\delta_{P_1}}{\alpha}\right]_{f(V_e)}\right\} - \left[\frac{\delta_{P_2}}{\delta_F}\right]_{f(\delta_F)}\delta_F \pm \frac{K_{B_p}\,\delta_{LG}}{1+\tau_2 s} + \frac{K_{A_p}\,\delta_F}{1+\tau_1 s}$$

flap $\Delta\alpha_{REF}$ correction term	flap drag correction term	landing gear simulation or compensation term	flap simulation term

Pitching moments produced by actuation of flaps, landing gear and the petals are controlled by generating signals to control δ_e. Figure 16 shows a block diagram of the control functions. The signals command elevator deflections so as to produce a zero net pitching moment whenever the flaps, landing gear, or petals are extended. If the pitching moment characteristics due to actuation of the flaps and the landing gear of a specific vehicle are to be simulated, the necessary functions can be programmed as indicated on the block diagram. These functions have the capability of sign reversals. All the functions are summed and drive the existing T-33 variable stability elevator servo. The equation describing the elevator servo control is as follows:

$$\delta_e = \pm\,\delta_F\left[\frac{\delta_e}{\delta_F}\right]_{f(\delta_F)} \pm\,\delta_p\left[\frac{\delta_e}{\delta_p}\right]_{f(\delta_p)} \pm\,\delta_{LG}\left[\frac{K_{B_e}}{1+\tau_2 s}\right] \pm\,\delta_{F_{SIM}}\left[\frac{K_{A_e}}{1+\tau_1 s}\right]$$

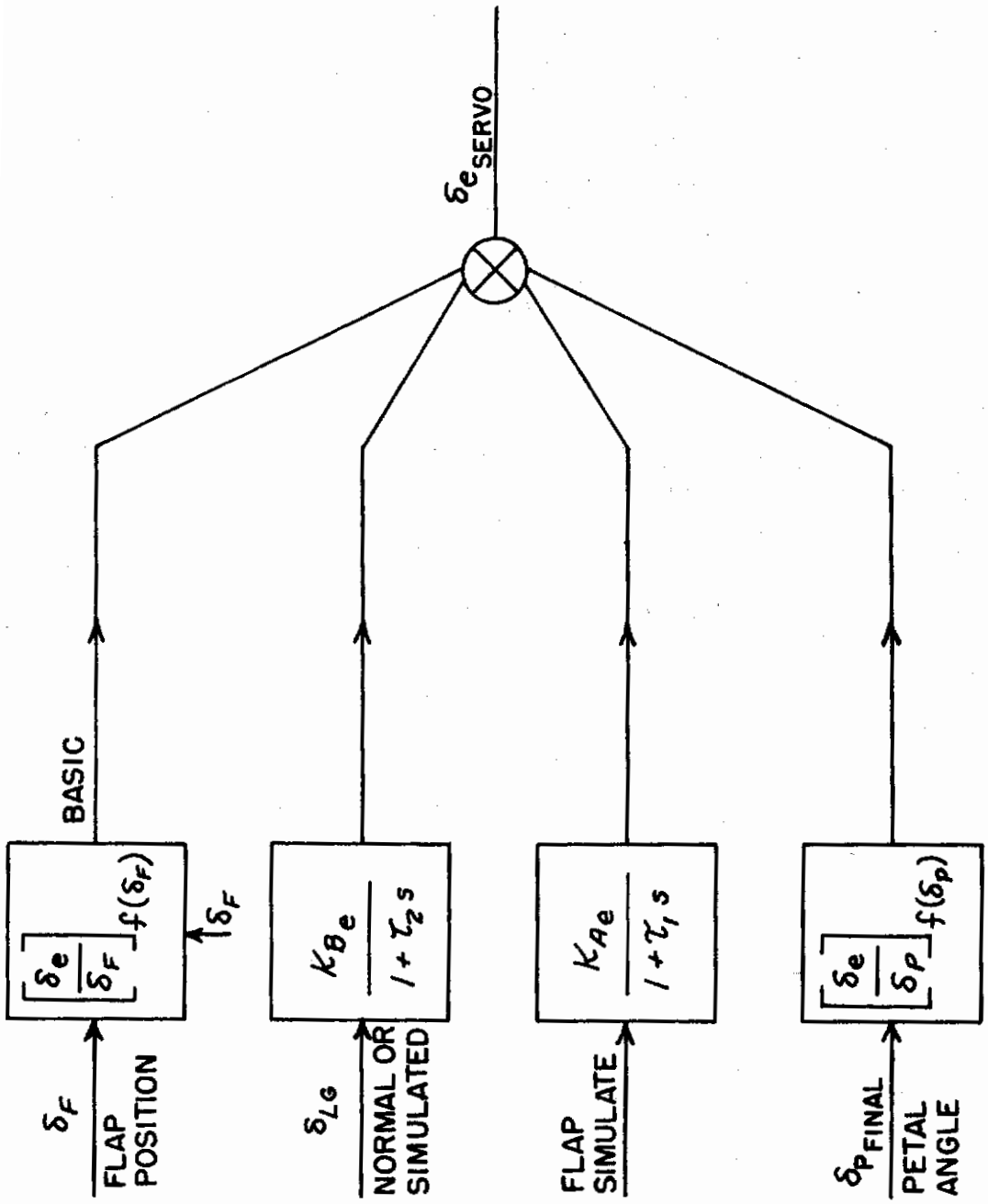

FIGURE 16 δ_e CONTROL BLOCK DIAGRAM

X_α, X_u Mode

A block diagram of the L/D system configuration that is used to produce changes in the stability derivatives X_α and X_u is shown in Figure 17. In this case, signals proportional to α and V_e can control the petal deflections. A trim control provides the initial setting of petal angle. The δ_p/α gain is adjustable in the cockpit, with a maximum gain of 10 degrees per degree obtainable. Another signal proportional to V_e can also control the petal deflections. The δ_p/V_e gain adjustment is provided also in the cockpit, with a maximum gain of 0.4 degrees per foot per second obtainable. The α and V_e signals are summed and the resultant signal drives the petal servos. An equation describing the operation of this mode is the following:

$$\delta_{p_{FINAL}} = \left(\frac{\delta_p}{\alpha}\right)\alpha + \left(\frac{\delta_p}{V_e}\right)V_e + \delta_{p_{TRIM}}$$

Pilot Control of L/D System

The safety pilot in the rear cockpit can manually control the petal deflections. Figure 18 shows this pilot's L/D control box. The manual control can be used to establish an initial petal position. The output of the computer can then be nulled with respect to the manual control setting, and the signal command switched over to the computer. Both left and right petal positions are indicated on the meters on the control panel. The null meter indicates the difference between the manually called-for petal position and the computer called-for petal position when the petals are driven manually. When the petals are operating in the computer mode, the null meter indicates the difference between the left and right petal position. If the petals are being operated from the computer signal, and it is desirable to disengage the L/D system, the pilot can rotate the manual control knob until it agrees with the existing petal angle. Then he can switch to manual control and rotate the knob to close the petals. A controlled disengage circuit is built into the system. The pilot can actuate the push button on the control panel at any time, and the petals will be driven closed at a rate determined by an RC circuit that has a time constant of approximately 5 seconds.

For safety of flight purposes a safety trip system removes excitation from the hydraulic dump solenoids whenever one or more of the following abnormalities occur:

1. The petal deflections differ by approximately 5° to 10° (adjustable)
2. Either petal rate exceeds approximately 30°/sec (adjustable)
3. The regulated power supply voltages are interrupted
4. The 400 cps carrier voltage is interrupted
5. The variable stability system automatic safety trip system operates.

Whenever the excitation to the hydraulic dump valves is interrupted, the valves will open and hydraulically short circuit the actuators, and the petals will close because of the drag loads on them. The L/D system can also be dumped manually by the pilot with the existing variable stability safety trip push buttons.

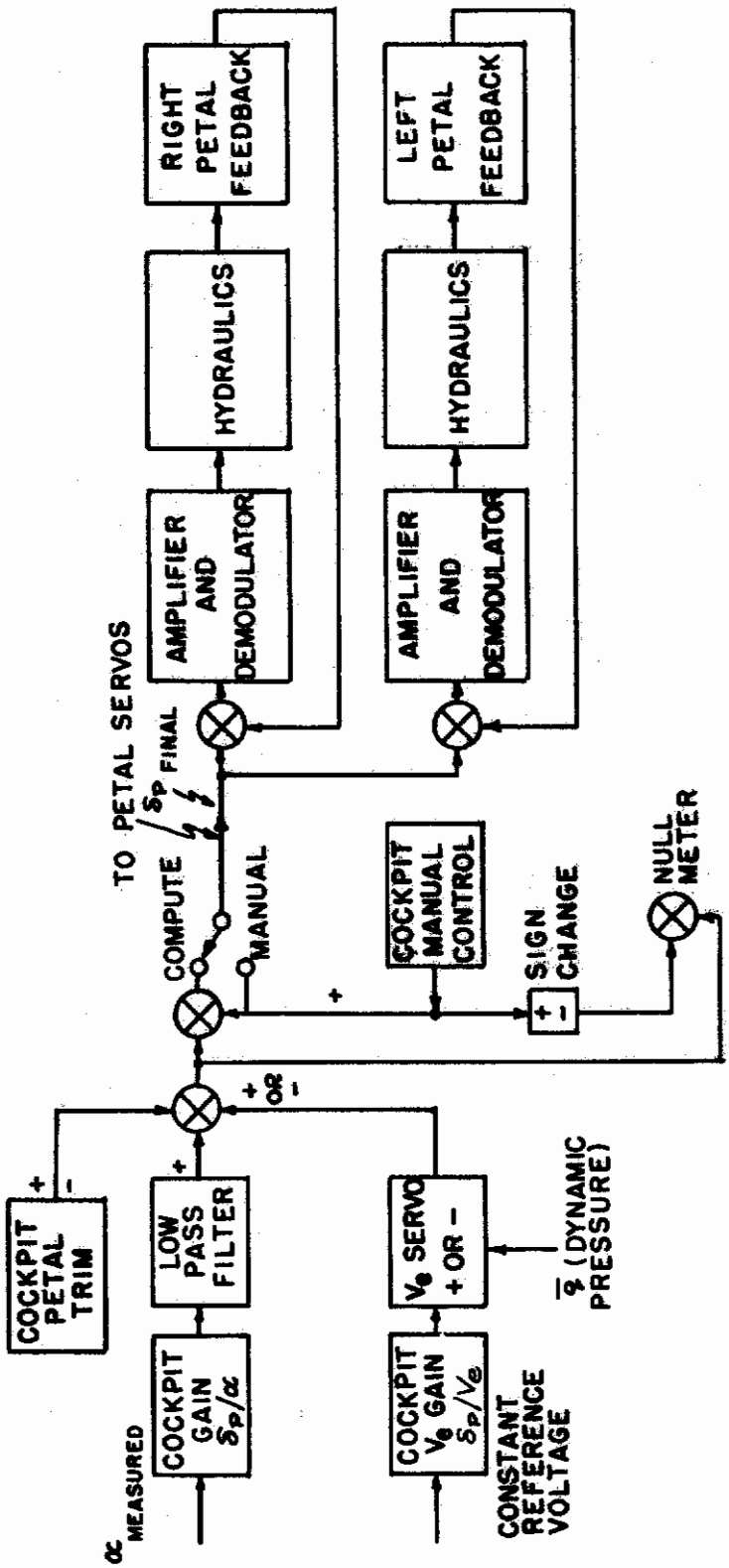

FIGURE 17 δ_p/α AND δ_p/V_e CONFIGURATION BLOCK DIAGRAM

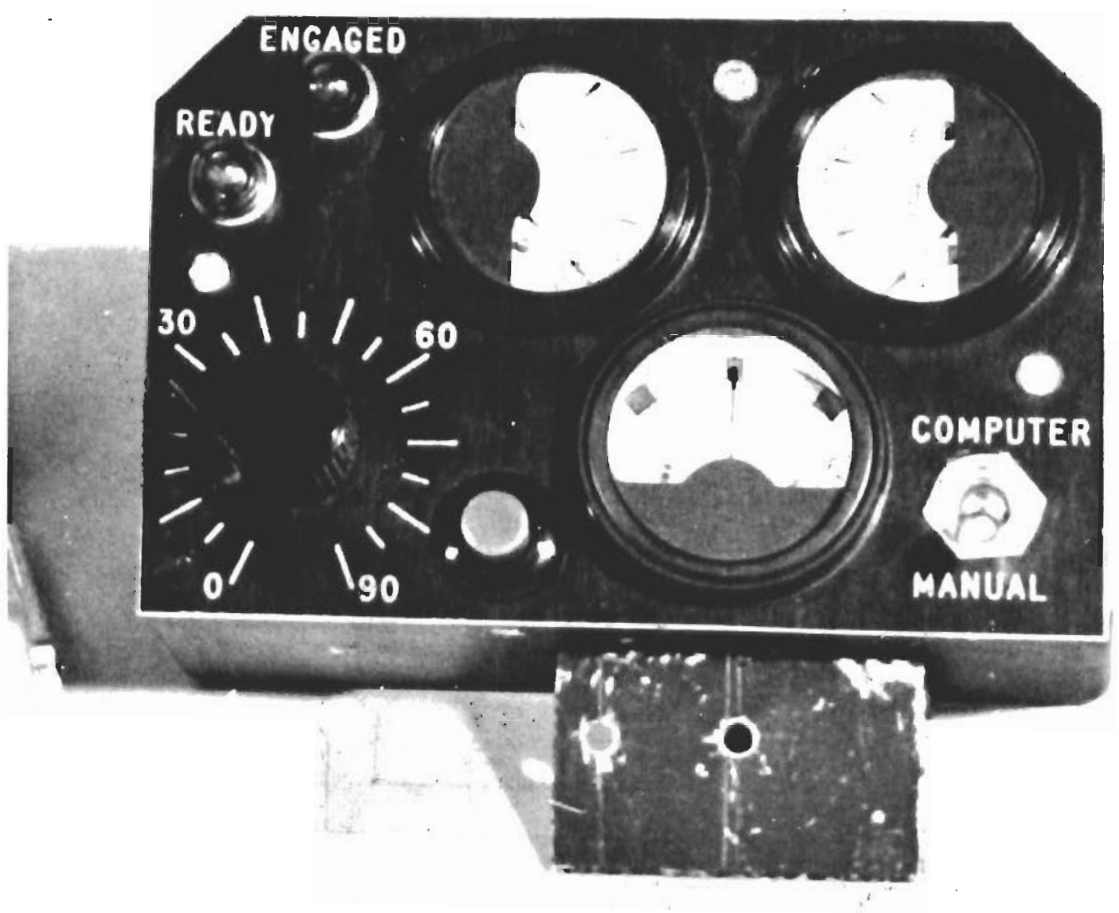

1948

FIGURE 18 PILOT'S CONTROL FOR L/D SYSTEM

B. MECHANIZATION

Sensors

The existing variable stability installation supplies the α (angle of attack) and $\bar{q}$ (dynamic pressure) signals used by the L/D computer. The V_e (equivalent velocity) signal required by the L/D computer is derived from the $\bar{q}$ signal. A measure of flap position is obtained from a pickup mounted on the flap linkage. The landing gear position signal available in the airplane is an indication of the "up lock" position. This signal is utilized to charge the RC circuit which simulates the gear drop time.

Computer

A simplified schematic diagram of the L/D computer is given in Figure 19. Gain, phase, time constant controls, etc., are called out on this schematic to allow convenient scale factor selection and function generator programming. The closed-loop stability of the transistorized amplifiers and the function generation technique provide the over-all computer accuracy. One percent precision resistors determine the amplifier closed-loop gains. The functions can be selected in two percent increments. Components were selected and circuitry designed to be insensitive to temperature and carrier frequency variations. Where this was impossible, thermistors were used to compensate for any gain or null change due to temperature. The computer was subjected to temperature variations from -55° centigrade to +55° centigrade and carrier frequency changes from 380 to 420 cps. Negligible changes in phase or gain were experienced. The low pass filter on the output of the α signal is required to eliminate frequencies from 18 to 40 cps that exist on the α vane output. This filter is flat to approximately 8.5 cps (180° phase) and attenuates 24 db/octave at frequencies above 8.5 cps. A lead-lag network in the filter provides zero phase shift up to 1 cps.

Function Generator

A schematic of a typical function generator is given in Figure 20. Multi-tapped carbon film potentiometers are servo driven by the parameter that controls the particular function. Three instrument servos, V_e, δ_F, and δ_p are contained in the system. Operation of the function generator is as follows: The function generator input is driven from a low impedance center-tapped transformer. The input is the voltage that is impressed across a string of fifty 10-ohm precision resistors which form a voltage divider of 2% steps of the total input voltage. If the function is both positive and negative, the center tap of the voltage divider is grounded. If the function is either always positive or always negative, one end of the string is grounded. The function is programmed by connecting each tap on the carbon film potentiometer to a point on the voltage divider that provides the proper gain ratio. Each tap corresponds to a specific value of V_e, δ_F, or δ_p. Linear interpolation results between the twelve tapped points. The potentiometer resistance is approximately 20,000 ohms which does not give any serious loading inaccuracy. The group of precision resistors at the right on Figure 20 are the input resistors to the summing amplifier. A specific resistor is selected to give the desired scale factor. This allows any function to be programmed over a reasonable range of the voltage divider.

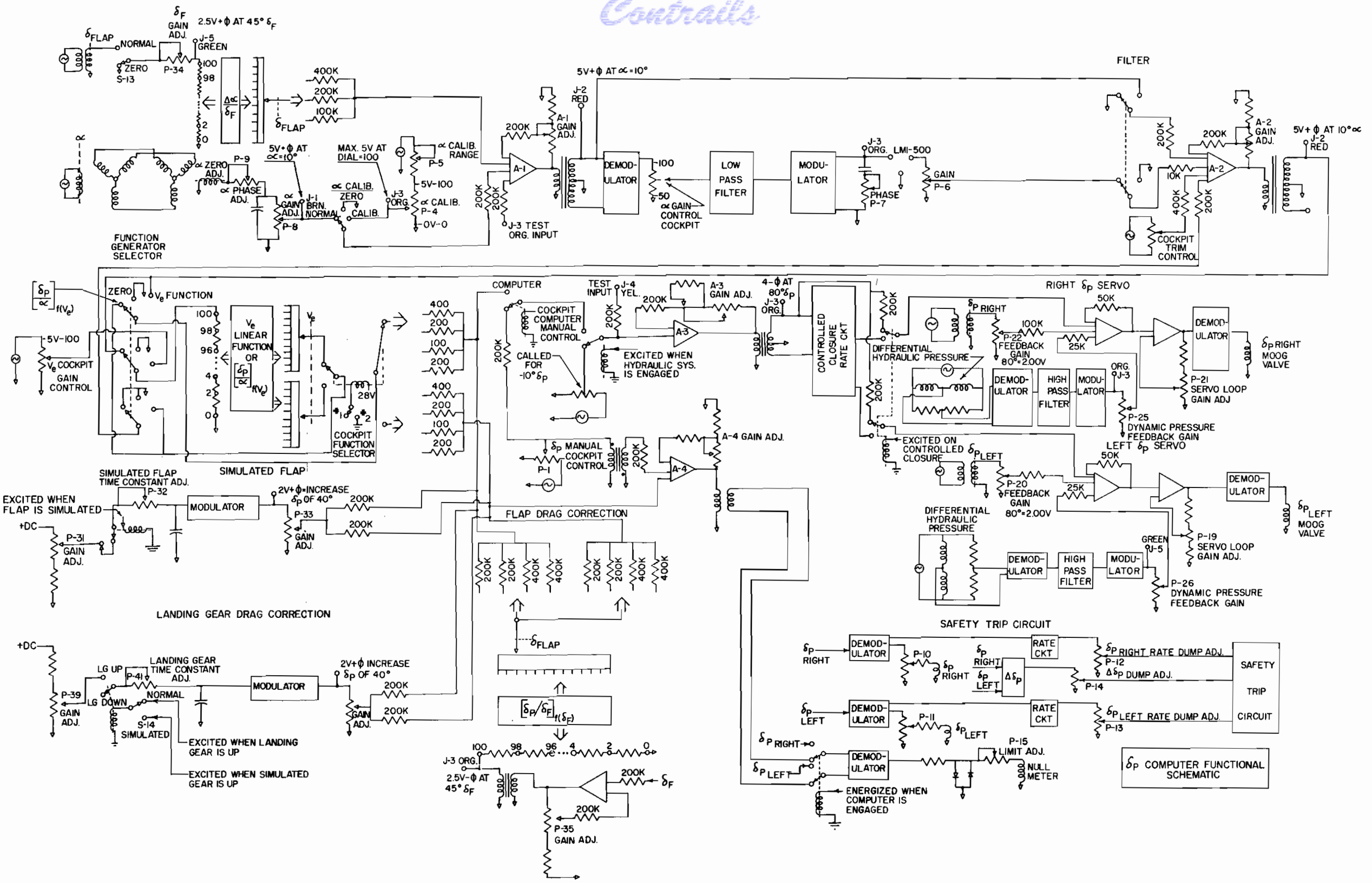

FIGURE 19 L/D COMPUTER SCHEMATIC

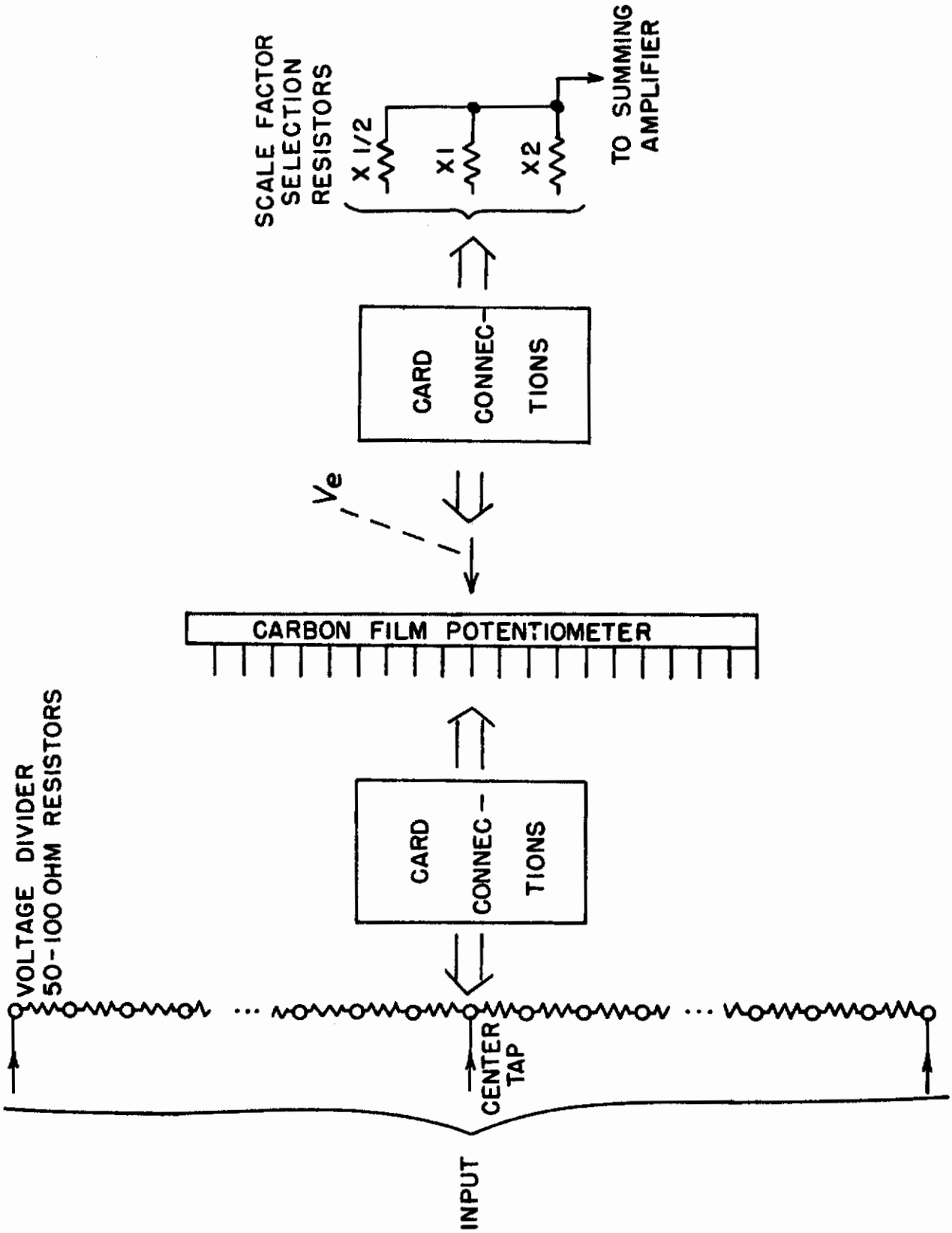

FIGURE 20 TYPICAL FUNCTION GENERATOR SCHEMATIC

Instrument Servos

To generate the functions noted on the block diagrams, Figures 15, 16 and 17, instrument servos providing positions equivalent to V_e, δ_F, and δ_p are required. The command signal to the V_e signal is $\bar{q}$, where $\bar{q}$ is proportional to V_e^2. A diagram of the V_e servo is shown in Figure 21. To provide this function, voltages from a resistor function card excite the feedback potentiometer in a nonlinear fashion. Thus, the servo position corresponds to specific values of V_e at each feedback potentiometer tap point, which are predetermined by the selection of voltages on the function card.

The δ_F and δ_p servos are linear follow-up servos of flap and petal position. They are similar to the V_e servo except that the function card is omitted. Frequency response tests of the three servos show that they are considerably better than required. The amplitude response is flat beyond 5 cps with a phase shift at 5 cps of less than 45 degrees. This well exceeds the frequency response requirements of δ_F and V_e changes and satisfies the frequency response requirements of δ_p changes.

Hydraulic Servo Electronics

Each petal servo, as shown on Figure 19, has a summing amplifier, a servo amplifier, and a demodulator to drive the hydraulic flow control servo valve. The δ_p computer signal and the servo feedback signal are summed. This combined signal drives the hydraulic servo until the combined signal becomes zero. The servo amplifier gain is selected to provide the desired servo response characteristics. To achieve a natural frequency of about 16 cps for the control loop, it was necessary to incorporate dynamic pressure feedback in each servo. Initial checkout of the hydraulic system showed that the petal servos, with petal extensions installed, were oscillatory with constant amplitude at approximately 17 to 20 cps whenever sharp step inputs were injected. An electrical pressure-transducer measures the differential pressure on each side of the hydraulic strut. This electrical signal goes through a high pass filter and is injected into the servo amplifier. The dynamic pressure feedback stabilizes the servo at high frequencies, yet has no effect on the servo static stiffness.

Automatic Safety Trip Circuit

Each petal hydraulic system contains solenoid-operated dump valves, around the strut, that must be excited for normal operation. Whenever the excitation to these solenoids is interrupted, the petals will close due to the airloads.

Figure 22 illustrates the automatic safety trip circuit developed to control excitation to the solenoid-operated valves.

An input transistor is required for each parameter (available as an electrical signal) desired to disengage the system if an excessive value is exceeded. Any number of input transistors can be paralleled in the circuit. When the system is operating normally, transistor T_o conducts, producing current i_o. The current i_o causes relay R_1 to energize and develops voltage E_o where $E_o = i_o R_o$. Whenever the voltage at any input exceeds E_o,

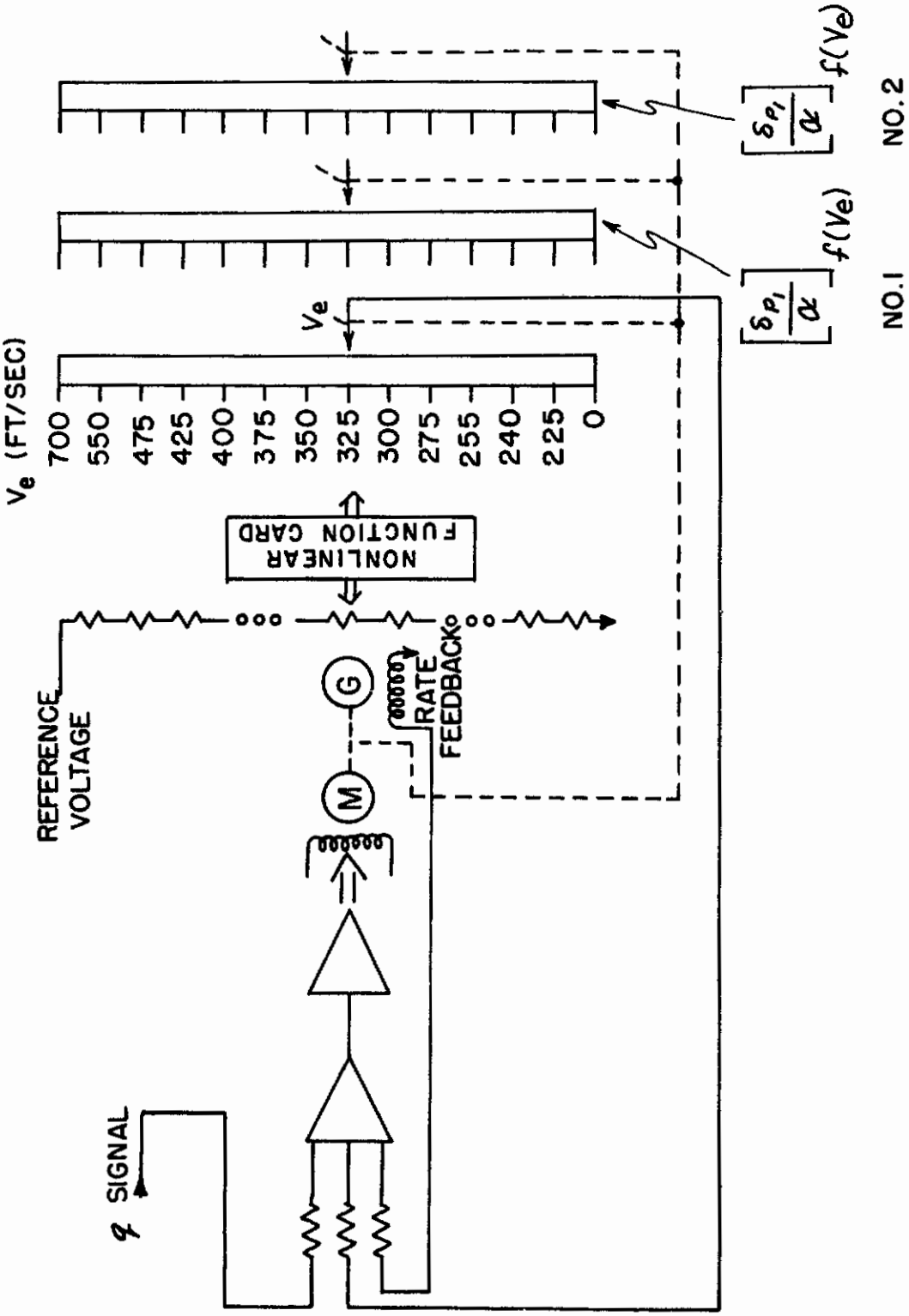

FIGURE 21 V_e SERVO SCHEMATIC

that specific input transistor switches to a conducting state. Transistor T_o simultaneously switches to its nonconduting state and relay R_1 drops out, thus disengaging the system. The circuit is "fail safe" in that if the 28 volt DC power is removed, the relay also drops out. This simple adaptation of the Schmitt Trigger Circuit requires very little power, has few components, is small in size and has proved to be extremely reliable.

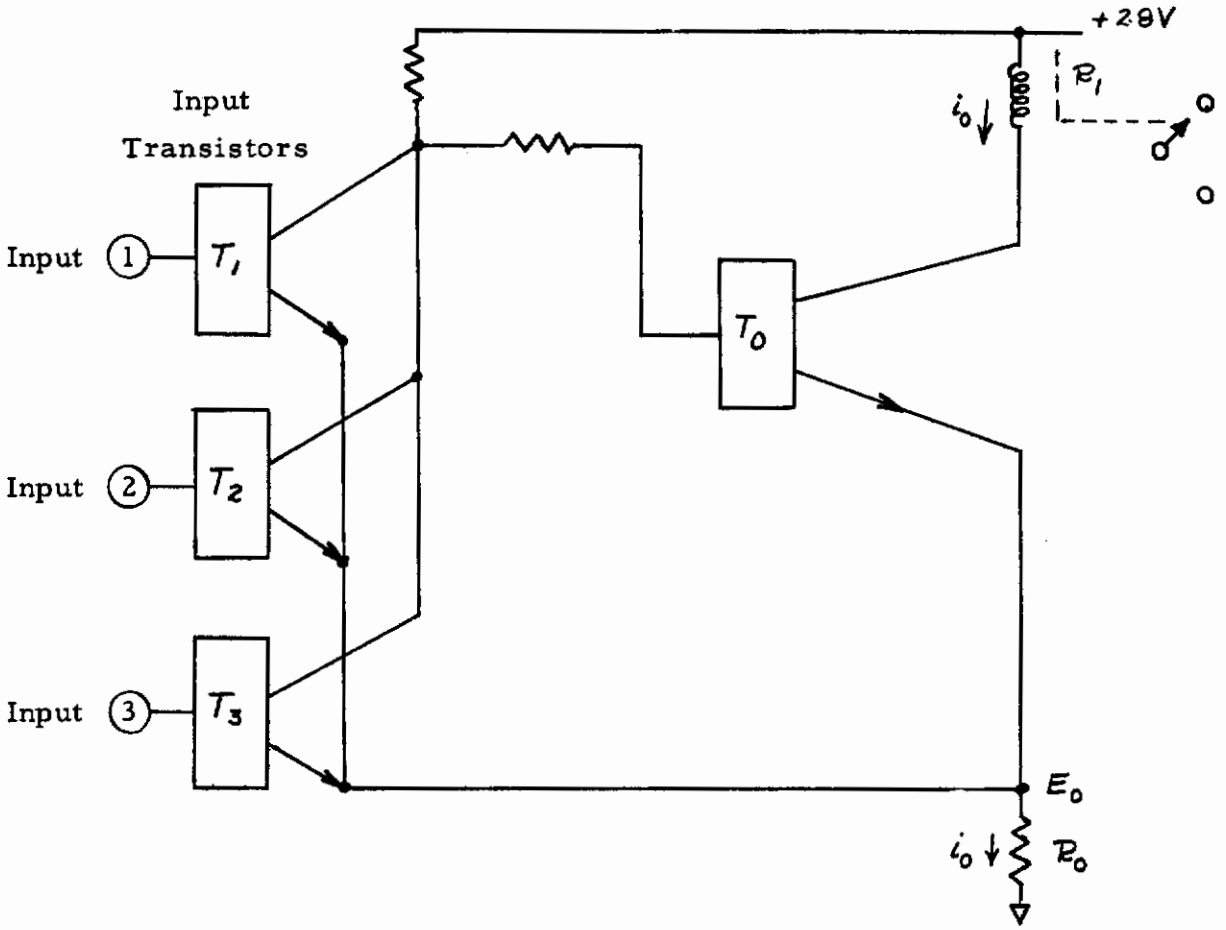

FIGURE 22 AUTOMATIC SAFETY TRIP CIRCUIT

SECTION 4
AERODYNAMIC CALIBRATIONS

Several aerodynamic calibrations of the L/D system are required. The drag of the petals, flaps, and landing gear must be determined. Because the landing gear and the flaps can be used with the petals, the pitching moment contributions of these must be accurately known. A flight test program was designed and conducted to obtain the data. The results of the tests are presented and discussed in this chapter.

Petal drag was determined from the flight test data by using Newton's Second Law of Motion, F = ma. First of all, trimmed straight and level flight was established with the petals closed. The petals were then opened, and the resulting deceleration measured with an accelerometer. This recorded deceleration, multiplied by the mass of the airplane, yields the drag that the petals produce. However, the analysis becomes complicated if changes in attitude, angle of attack and velocity occur. Such changes (though small) do occur because the airplane does not remain in precise trim, and because the velocity drops due to deceleration. Therefore, it was necessary to develop the perturbation equation to account for these changes.

The perturbation equation was obtained by subtracting the x-force equation of motion for the reference flight condition from the x-force equation of motion for the petals-open condition. The equation of motion in the body axis system for the reference flight condition is:

$$\Sigma X_b : -L\sin\alpha_o + T\cos\xi - D\cos\alpha_o - mg\sin\theta_o = 0$$

where L and D are the wind axis lift and drag forces respectively; α_o and θ_o are reference angle of attack and pitch angle respectively; T is the thrust; ξ is the angle between the thrust vector and the x-body axis; and mg is the weight of the airplane. The equation of motion after the petals are opened is:

$$\Sigma X_b : -L\sin(\alpha+\alpha_o)+T\cos\xi - D\cos(\alpha+\alpha_o) - mg\sin(\theta+\theta_o) - D_p\cos(\alpha_o+\alpha) = ma_x$$

where α and θ are perturbation quantities; D_p is the drag of the petals; and a_x is the resulting acceleration. Note that the change in flight path angle is included. Therefore, after standard small angle assumptions are made, subtracting the petal-open equation from the reference equation yields the perturbation equation:

$$\Sigma X_b : \alpha L - \theta mg - D_p = ma_x$$

Extreme care is required when using this equation. In any particular flight test evaluation the relative magnitudes of the small quantities must be assessed before any small quantities are discarded. For example, the terms αL and θmg will cancel under certain conditions, but care must be used to verify that these conditions exist before any terms are dropped.

The drag of the petals, for various petal angles, obtained by the above procedure is shown in Figure 23. A linear variation of petal drag with petal angle is seen to exist throughout the full range of petal angles, although this

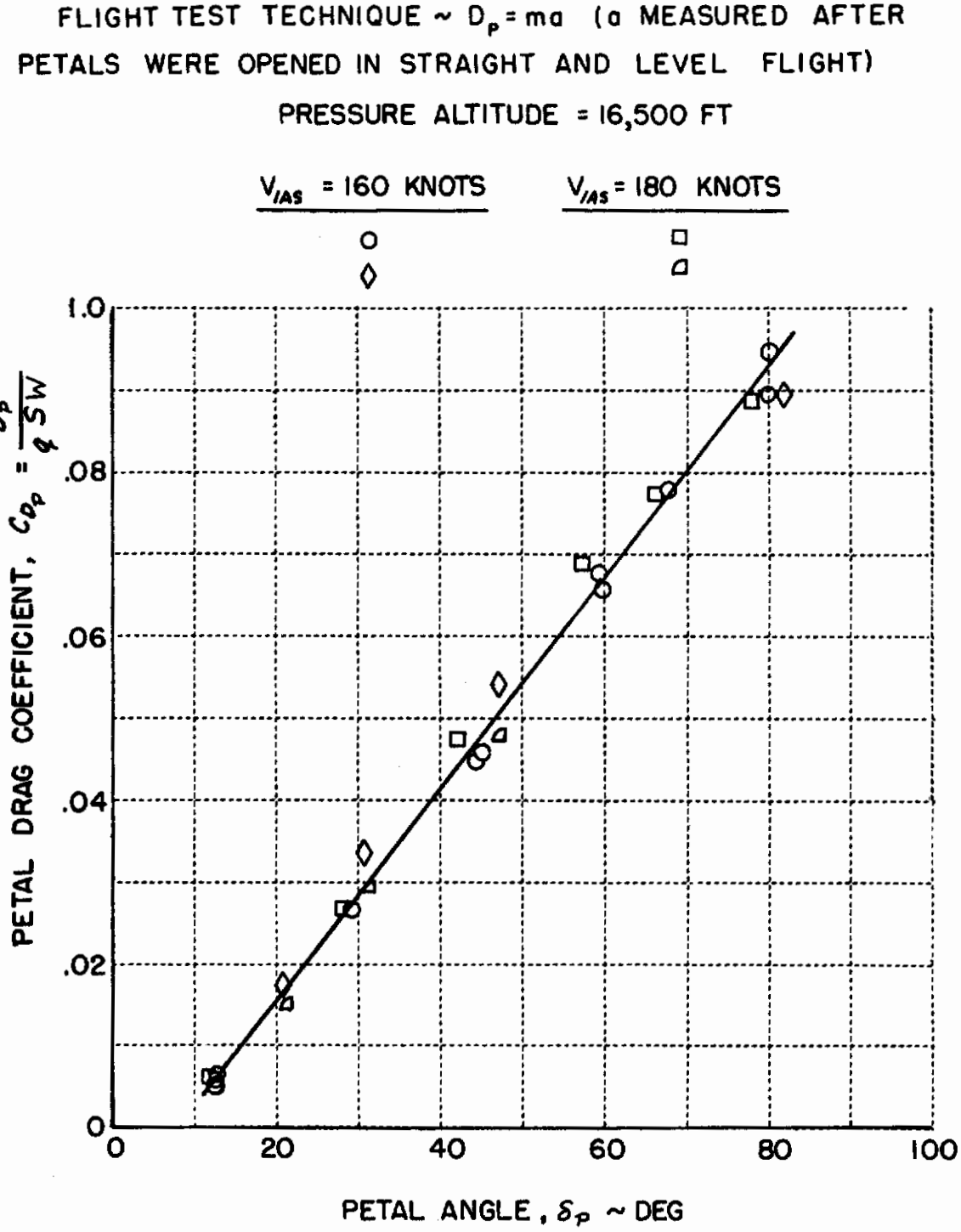

FIGURE 23 DRAG OF THE PETALS

was not expected on the basis of wind tunnel tests (see Figure 5). Data is presented at 160 and 180 knots and there is no indication that the drag coefficient of the petals has changed; therefore, it is implied that an angle of attack change from approximately 4.5 to 6.5 degrees, which is the change in trim angle of attack for speed changes from 180 knots to 160 knots, has not significantly changed the drag coefficient of the petals.

A second procedure was also used to measure petal drag. In this case, after the petals were opened, a steady state of descent was established at the same velocity and power setting as the trimmed, level-flight reference condition. The flight path angle was then measured and used to compute petal drag. The results appear in Figure 24. The straight line shown in Figure 24 is the same straight line that appears in Figure 23. Good agreement is seen to exist from both flight test techniques. The increased scatter in Figure 24 is attributed to the difficulty in measuring the flight path angle precisely and the difficulty in establishing a well-stabilized trim.

Wind tunnel tests indicated that the pitch moment produced by the petals would be negligible. However, the experiments to determine petal drag revealed that the petals do produce a significant pitching moment. Therefore, it was necessary to determine the change in elevator angle required to reestablish trim when the petals were opened. The elevator angle changes were made with the variable stability system to keep the elevator trim tab from influencing the results.

The required change in elevator angle for petal angle is shown in Figure 25. Maximum elevator angle required to trim occurs at approximately 45° of petal angle, while the change in elevator angle required at both zero and full petal deflection is approximately zero. Furthermore, the large variation of change in elevator angle with velocity apparently indicates that the compensation required is a function of initial trim angle of attack as well as petal angle.

The flaps must be lowered during a simulated L/D profile to attain low values of effective L/D at low indicated airspeed. However, it is undesirable for the evaluation pilot to sense the deceleration due to lowering flaps. Therefore, flap drag must be compensated by a reduction in petal drag. To establish the petal angle change required to produce no net increase in drag, the drag of the flaps for various flap deflections was determined from a brief flight test.

The flight test consisted of establishing trimmed straight and level flight at 16,500 feet pressure altitude and 160 knots IAS with the flaps deflected at some angle. The flaps were then retracted and the petals deflected until the reference flight condition was again attained with constant thrust. Thus, the petal drag was equal to flap drag during the reference flight condition. Since petal drag was previously established, as shown in Figure 23, flap drag could be calculated from the change in petal position.

Figure 26 illustrates flap drag determined in this manner; it is seen to be nearly linear with flap deflection angle. Full flap yields an increase in drag coefficient of 0.055. An auxiliary scale on the figure indicates the petal angle change required to produce drag equal to the corresponding flap drag. If the flaps are fully lowered then the petals must be retracted 50° to maintain the same reference total drag.

FLIGHT TEST TECHNIQUE ~ CHANGE IN FLIGHT PATH ANGLE MEASURED AFTER PETALS WERE OPENED.

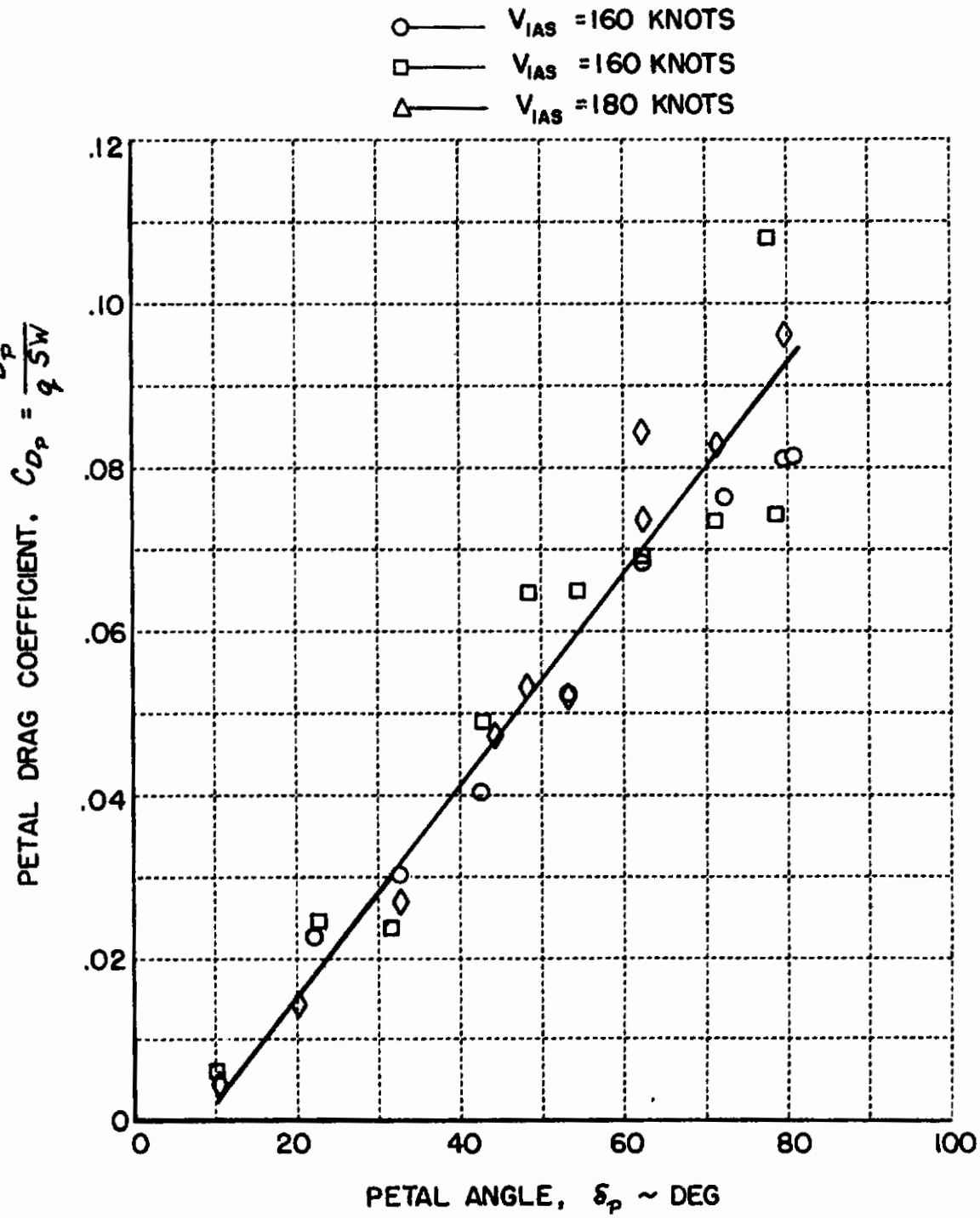

FIGURE 24 DRAG OF THE PETALS

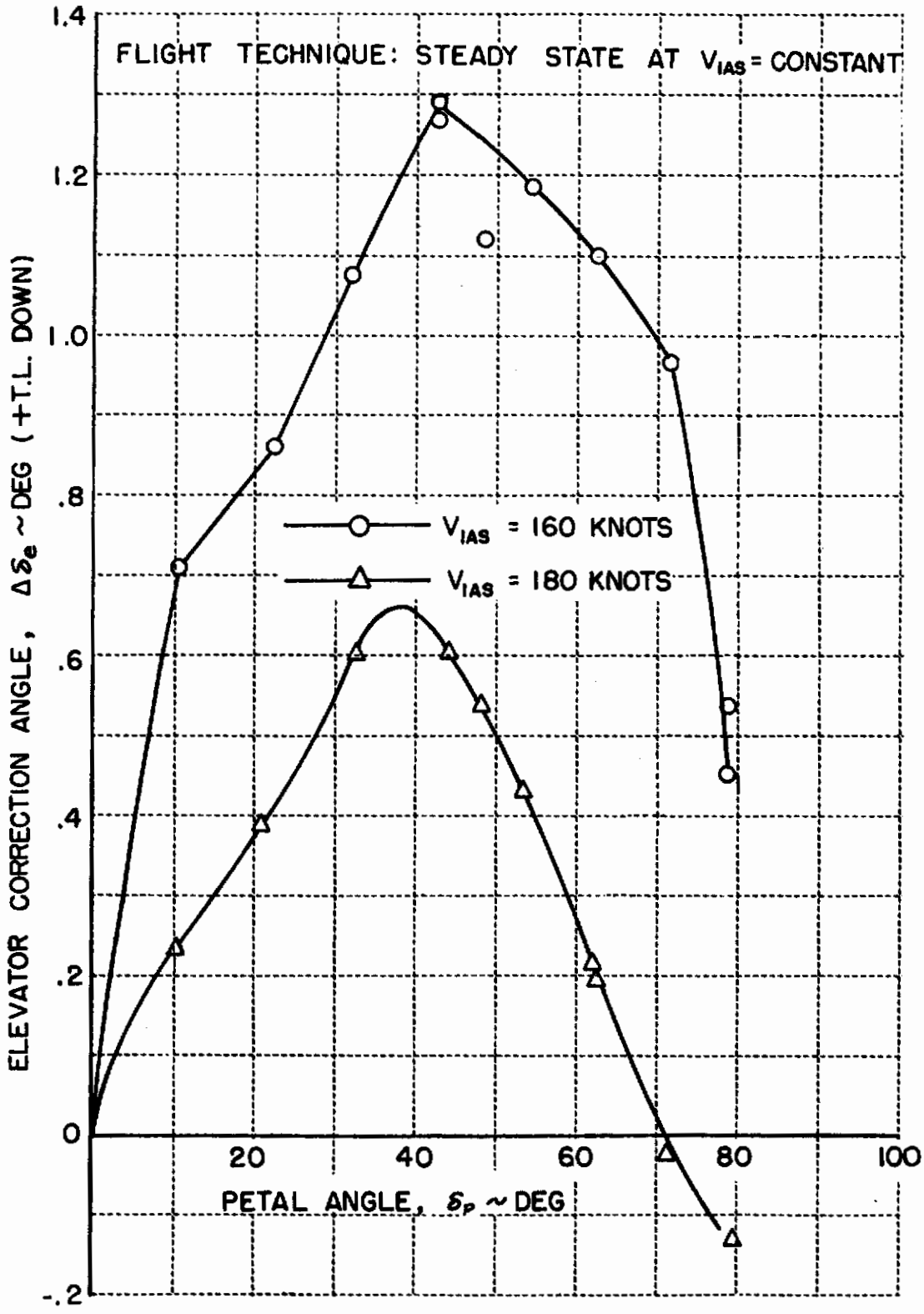

FIGURE 25 ELEVATOR ANGLE CORRECTION TO TRIM

The change in zero-lift angle of attack as a function of flap deflection was also obtained from flight testing because only full and take-off flap data were available. The angles of attack were recorded for stabilized straight and level flight at 160 knots indicated airspeed for various angles of flap deflection. These angles were compared to the angle of attack for zero flap angle and thus Figure 27 was generated.

The flap drag flight test also provided the data from which the elevator angle required to trim out the flap pitching moment is determined. The elevator compensation for the pitching moment that is produced by the flaps is shown in Figure 28.

Both the landing gear and the speed brakes are used to achieve the low values of effective L/D. The drag and pitching moment so produced was obtained by the same procedure used in the case of the flaps. The petal angle to produce the same drag as the landing gear at 160 knots indicated airspeed was 30°, while 25.4° was required to produce the equivalent drag of the speed brake. These petal angles correspond to drag coefficients of 0.028 and 0.022 respectively. The elevator angles required to maintain the same reference flight condition after lowering of landing gear and speed brake were 0.795° and 0.559° respectively.

The drag data for the various devices are used to show the obtainable values of effective L/D in a series of summary graphs; Figures 29 through 34. A family of curves is plotted that shows the drag force per petal as a function of indicated airspeed for a given petal angle. This family of curves was generated from the petal drag polar, Figure 23. A second family of curves shown in the summary graphs indicates the drag per petal required to achieve a given effective L/D as a function of indicated airspeed. All the data used to establish the drag was determined from the series of flight tests previously described with the exception of the drag for the clean airplane. The drag of the clean T-33 was obtained from Reference 10.

Because it will be desirable to use different configurations and flight conditions in the various L/D system experiments, the effects of landing gear, flap, speed brake positions, altitude, and gross weight are shown in the summary graphs. Figure 29 shows the effective L/D's obtainable for the clean airplane plus petals at sea level and a gross weight of 13,000 lb. The engine thrust is assumed to be 600 pounds, which corresponds to approximately 55% engine rpm at sea level. It is noted that an effective L/D of less than 4 can be obtained only at indicated airspeeds greater than 203 knots. This fact indicates the importance of the landing gear, speed brake and flaps if lower $(L/D)_e$ is desired. The next four summary plots, Figures 29, 30, 31 and 32 show the effects of altitude and configuration variations.

The variation of effective L/D ratio with altitude is a result of thrust variation. The thrust at 55% rpm is 600, 300, and 200 pounds at sea level, 10,000 ft, and 20,000 ft, respectively. With the speed brakes extended and a gross weight of 13,000 pounds, an effective L/D ratio of 4 can be obtained at 187 knots at sea level, whereas an effective L/D equal to 4 can be obtained at 178 knots at 10,000 ft, and 175 knots at 20,000 ft. A comparison of Figures 29 and 30 shows clearly the importance of using the dive brakes in conjunction

with the petals. By opening the dive brakes, the airspeed was reduced from 203 to 187 knots to achieve an effective L/D of 4.

Figures 33 and 34 illustrate the lowest values of effective L/D ratio that are obtainable at sea level with the L/D system. In these figures values of effective L/D are shown with the flaps and landing gear extended at the respective limit speeds. The limit speed for the landing gear is 192 knots. The flaps may be extended 50% at 192 knots and 100% at 174 knots. The calculations shown are based on the assumption that the flaps are lowered linearly with indicated airspeed in the region from 192 to 174 knots. The large effects of the landing gear and flaps in producing drag is apparent from the large discontinuity in the curves. The effect of gross weight is also seen from a comparison of Figures 33 and 34. In general, an increase in gross weight increases the effective L/D at a given indicated airspeed. Furthermore, as the effective L/D decreases gross weight changes become more important. It is seen that an effective L/D of 4 can be obtained for airspeeds above 130 knots for 12,000 pounds gross weight and above 137 knots for 14,000 pounds.

The summary graphs may be conveniently used to determine the functions for any L/D profile that is to be evaluated. If the L/D profile vs. velocity is superimposed on the appropriate summary graph, then the petal angle vs. velocity function can be read directly. This function is then programmed in the function generator. It is noted that although many calibrations were required to determine the various functions for the L/D system, only the petal angle vs. velocity function must be changed from time to time. The compensating functions for drag, pitching moment, and angle of attack from the flaps, landing gear and petals will not fluctuate.

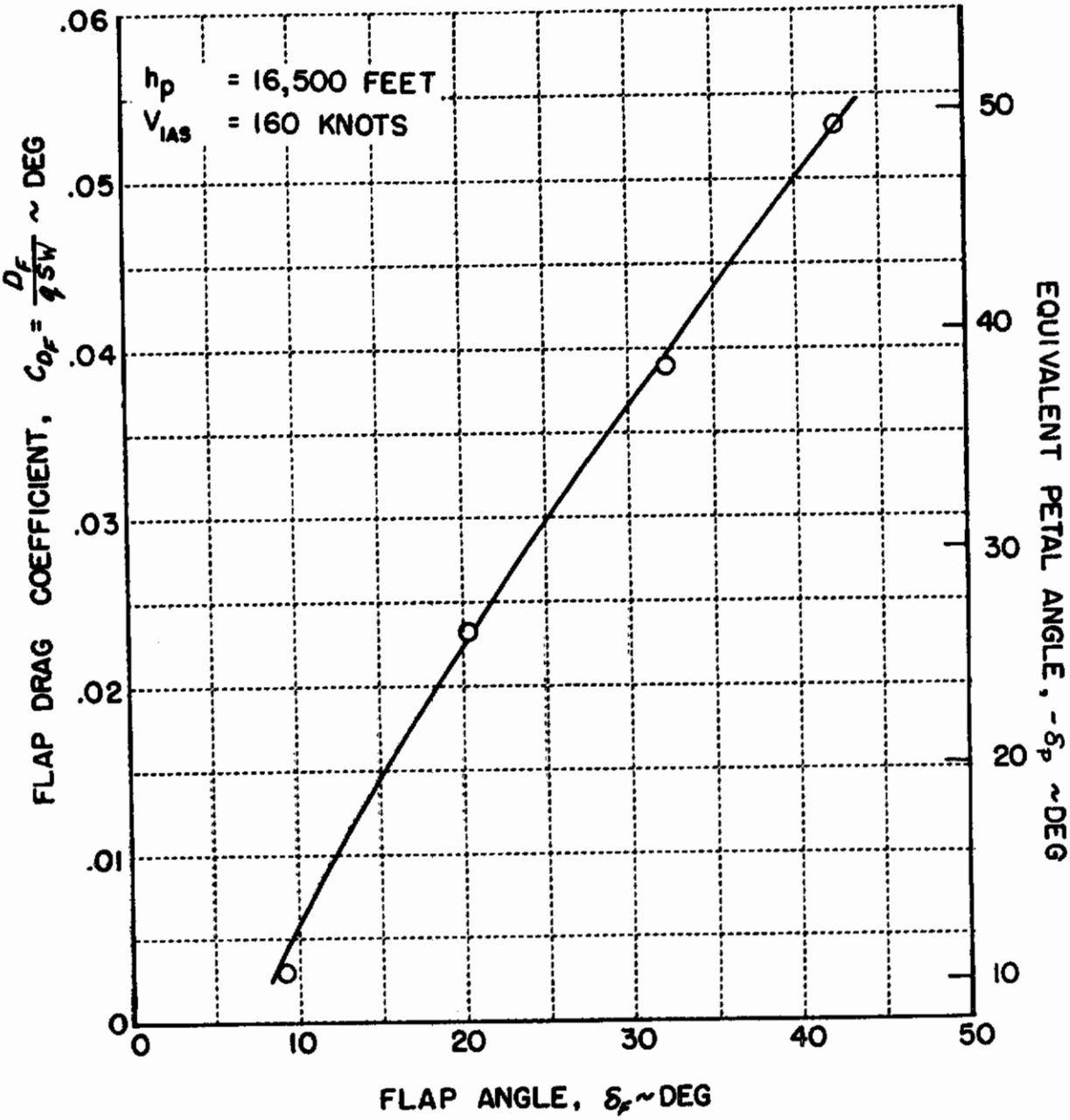

FIGURE 26 DRAG OF THE FLAPS

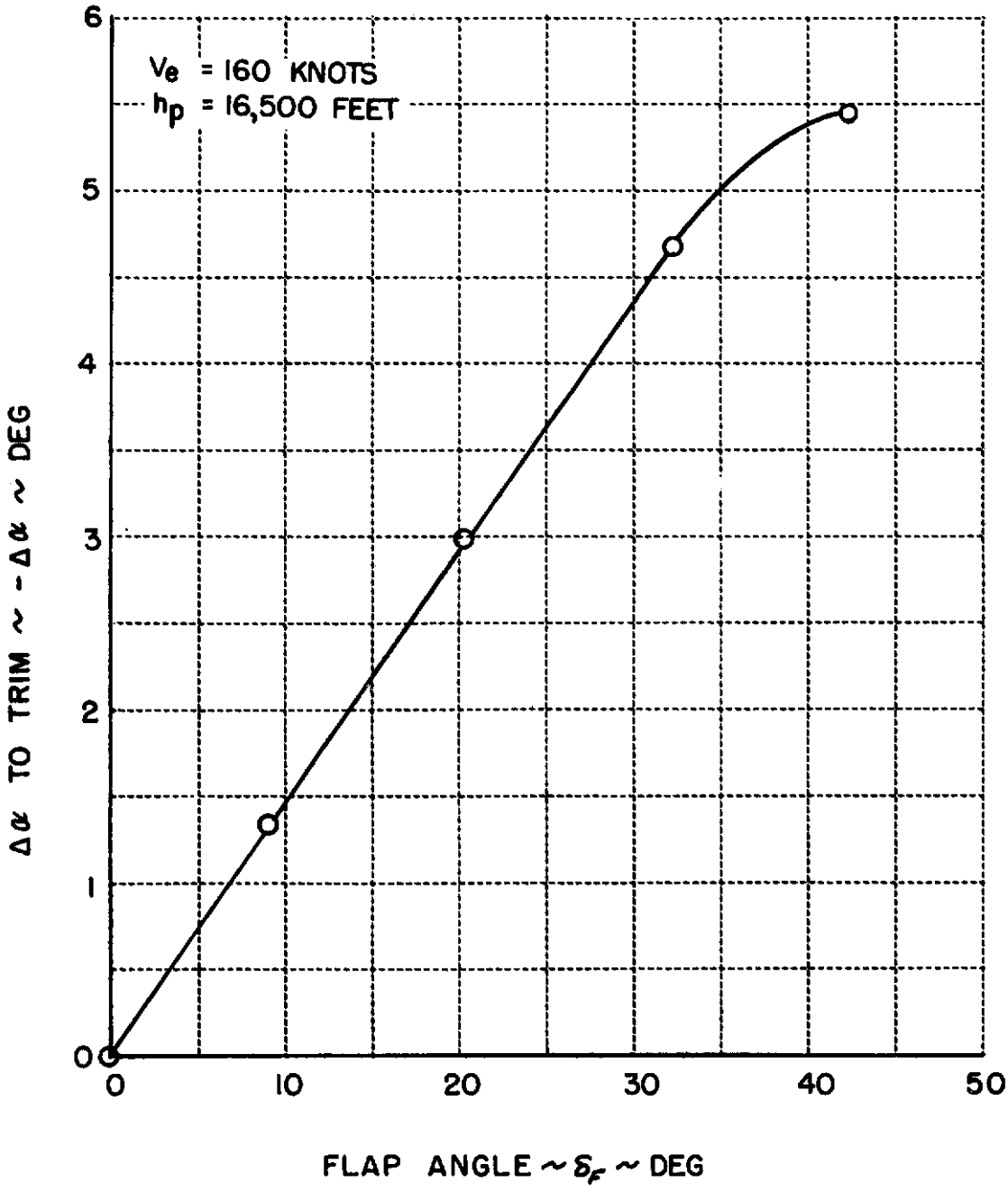

FIGURE 27 CHANGE IN ZERO-LIFT ANGLE OF ATTACK AS A FUNCTION OF FLAP DEFLECTION

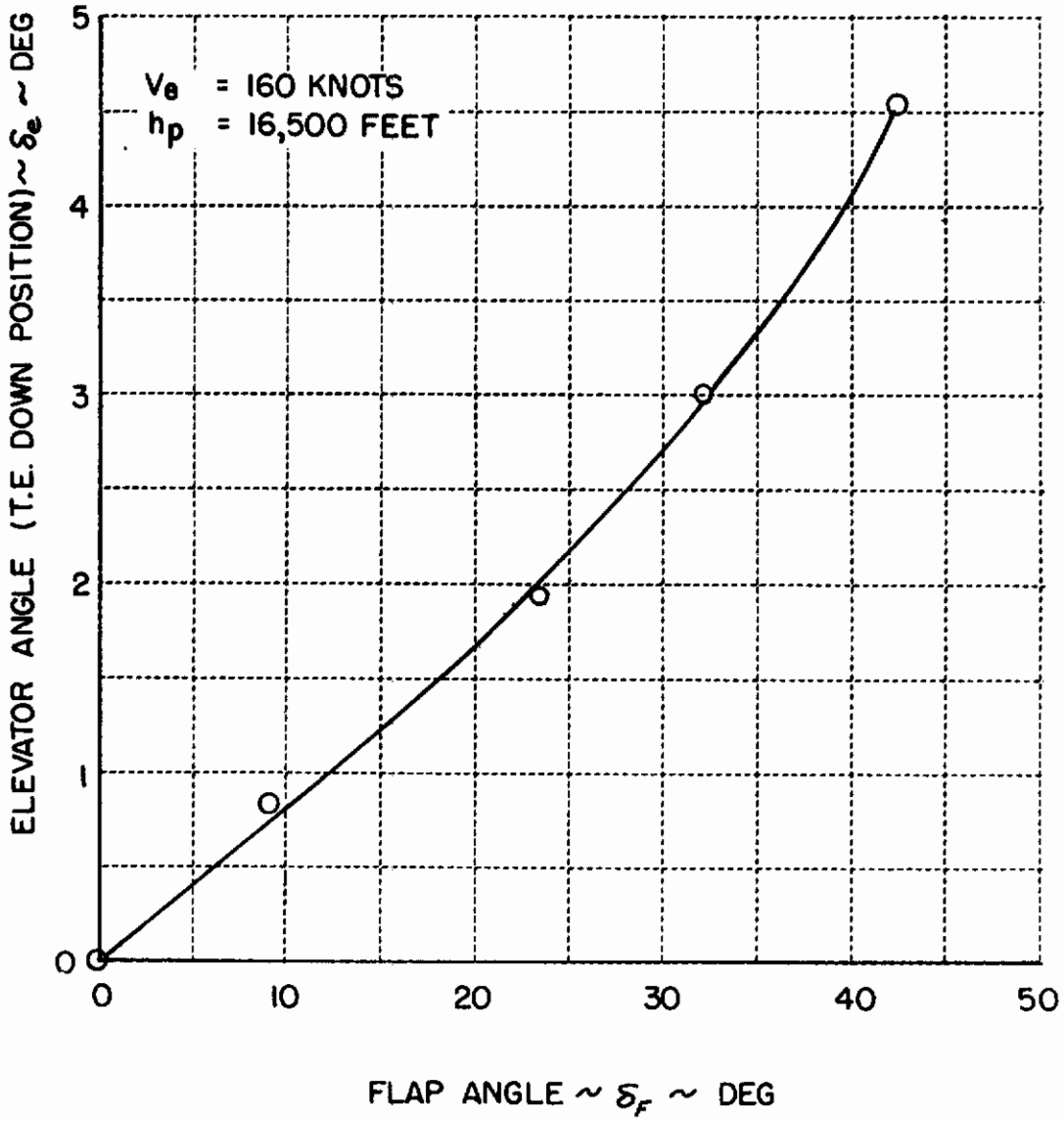

FIGURE 28 ELEVATOR ANGLE CORRECTION FOR FLAP DEFLECTION

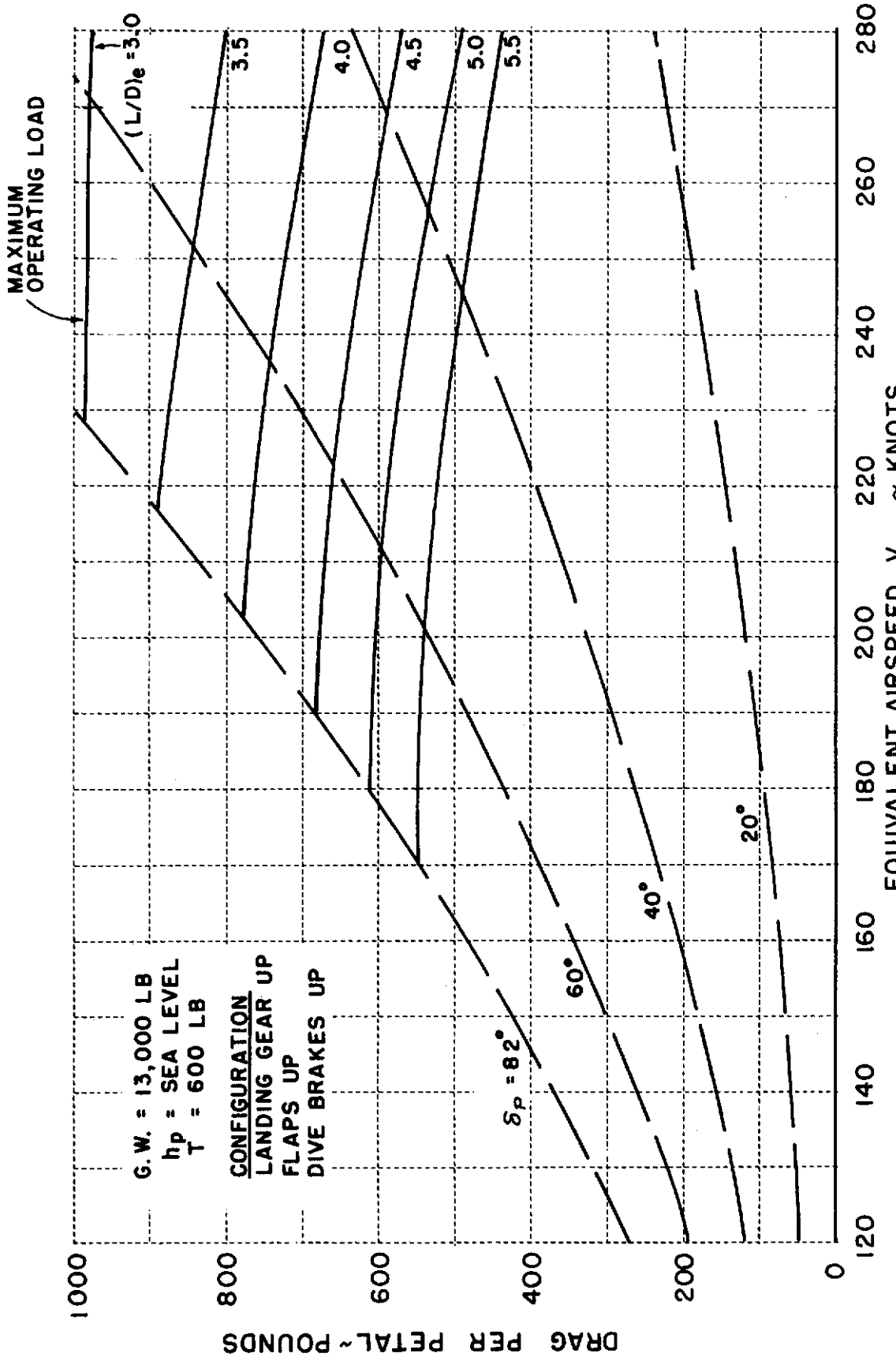

FIGURE 29 L/D CALIBRATION CHART

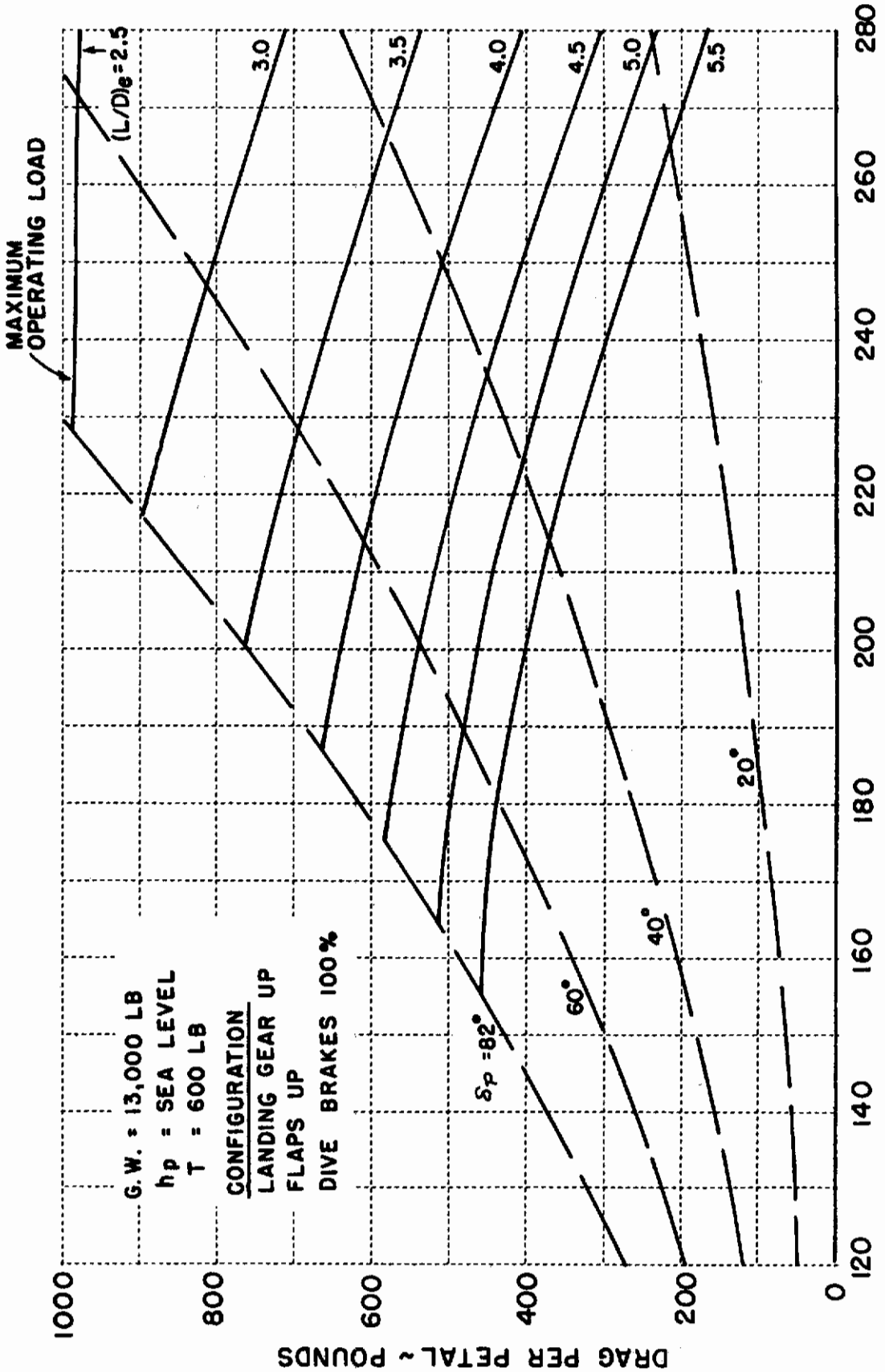

FIGURE 30 L/D CALIBRATION CHART

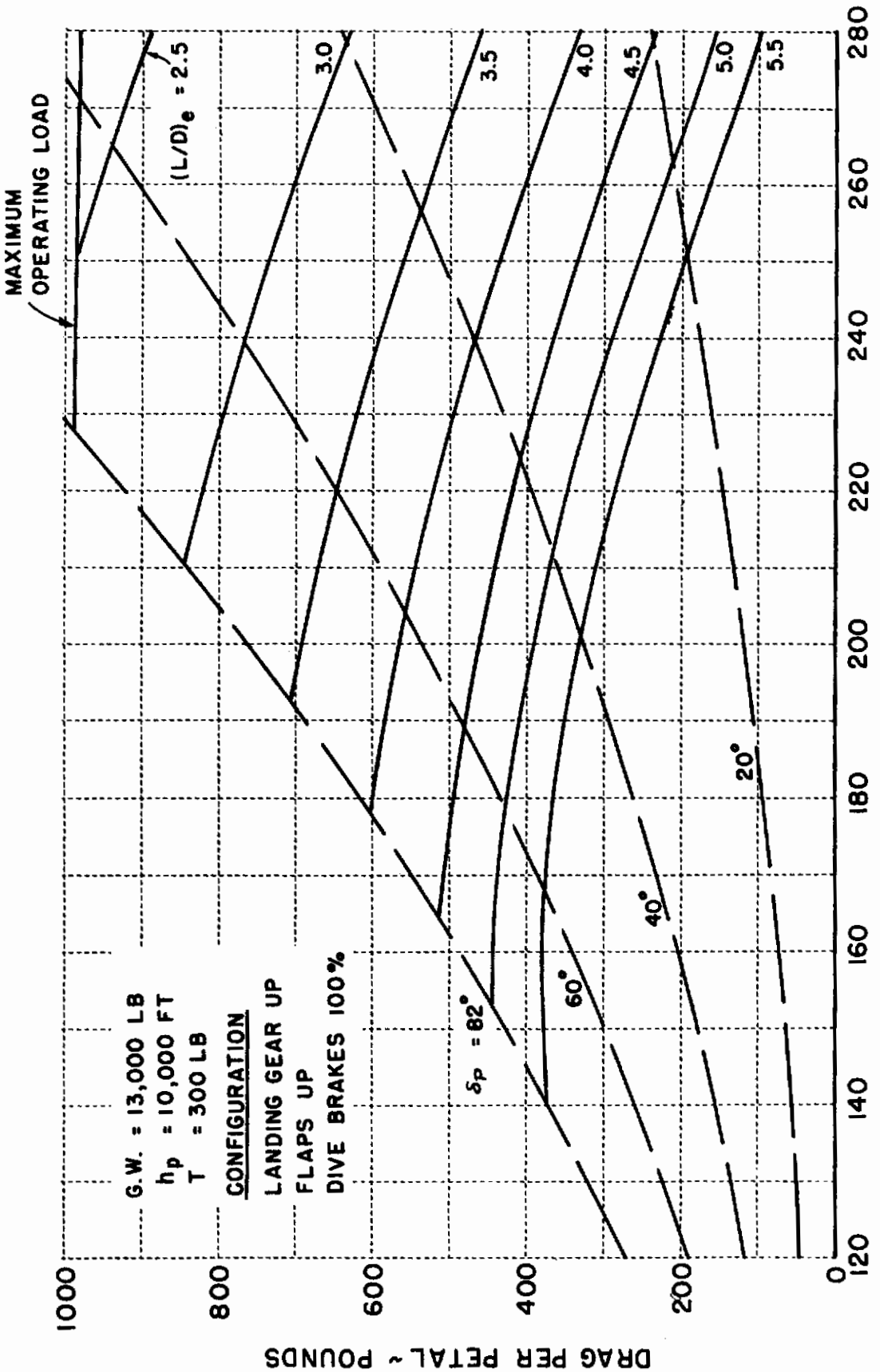

FIGURE 31 L/D CALIBRATION CHART

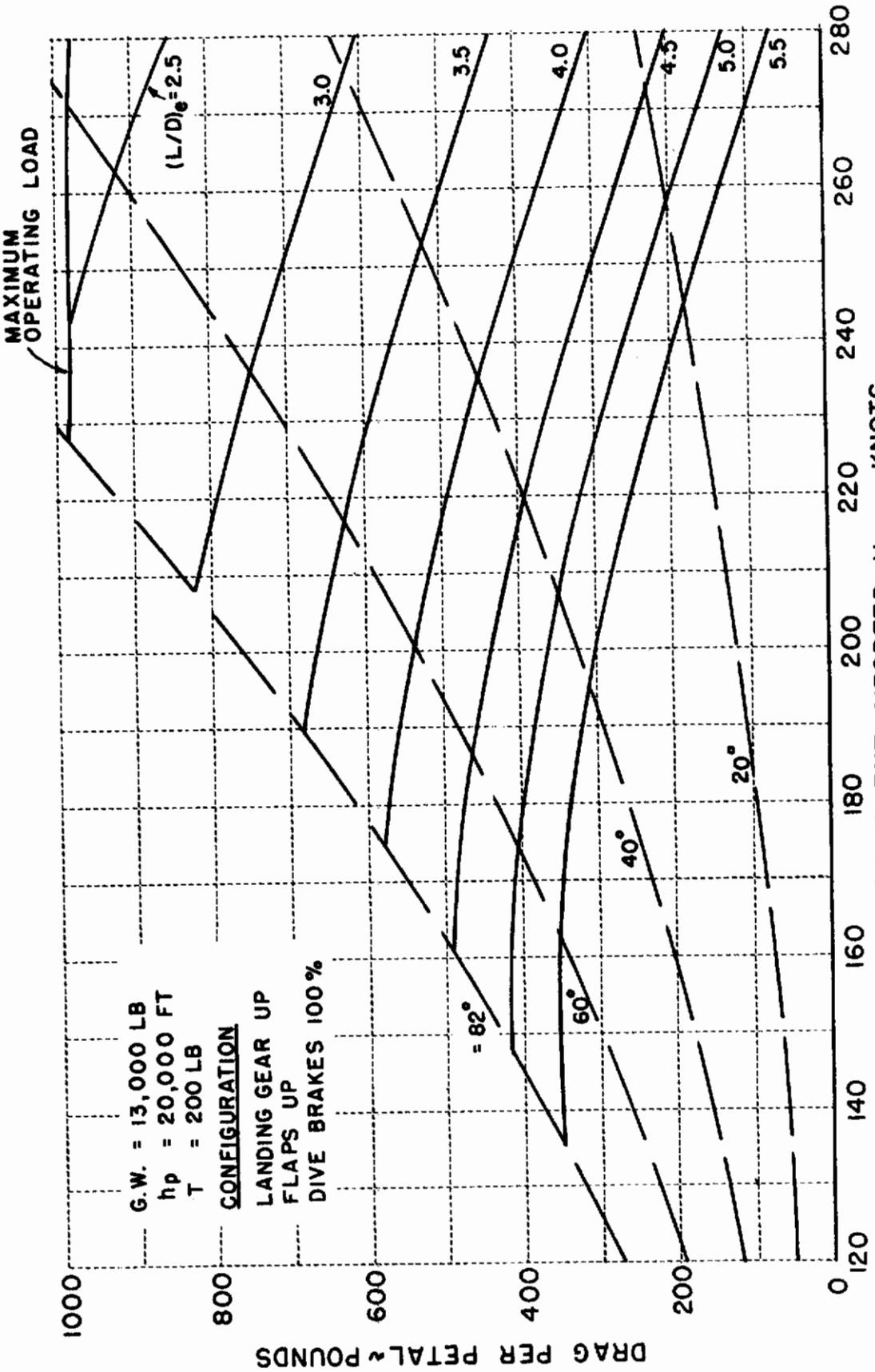

FIGURE 32 L/D CALIBRATION CHART

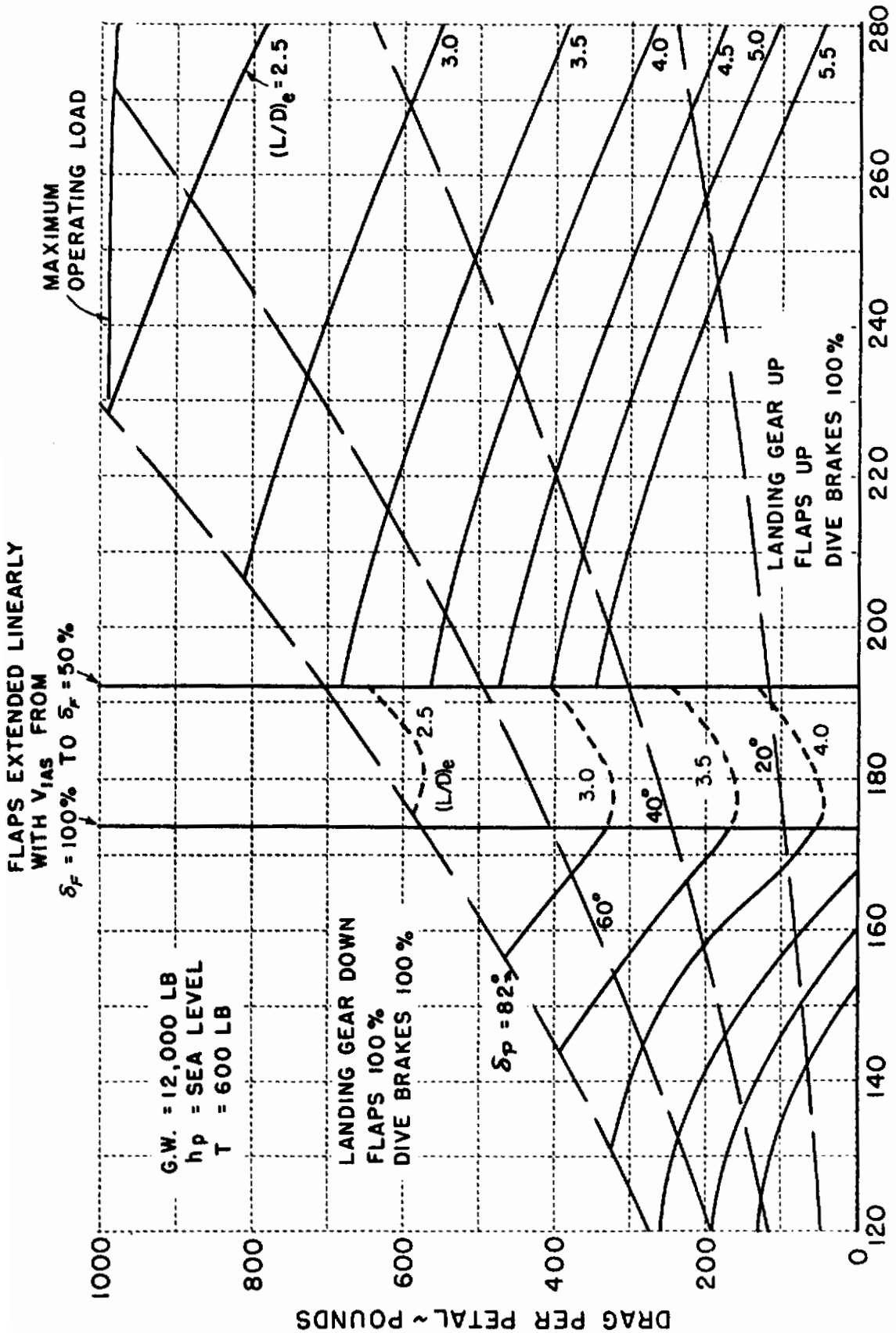

FIGURE 33 SEA LEVEL SUMMARY PLOT

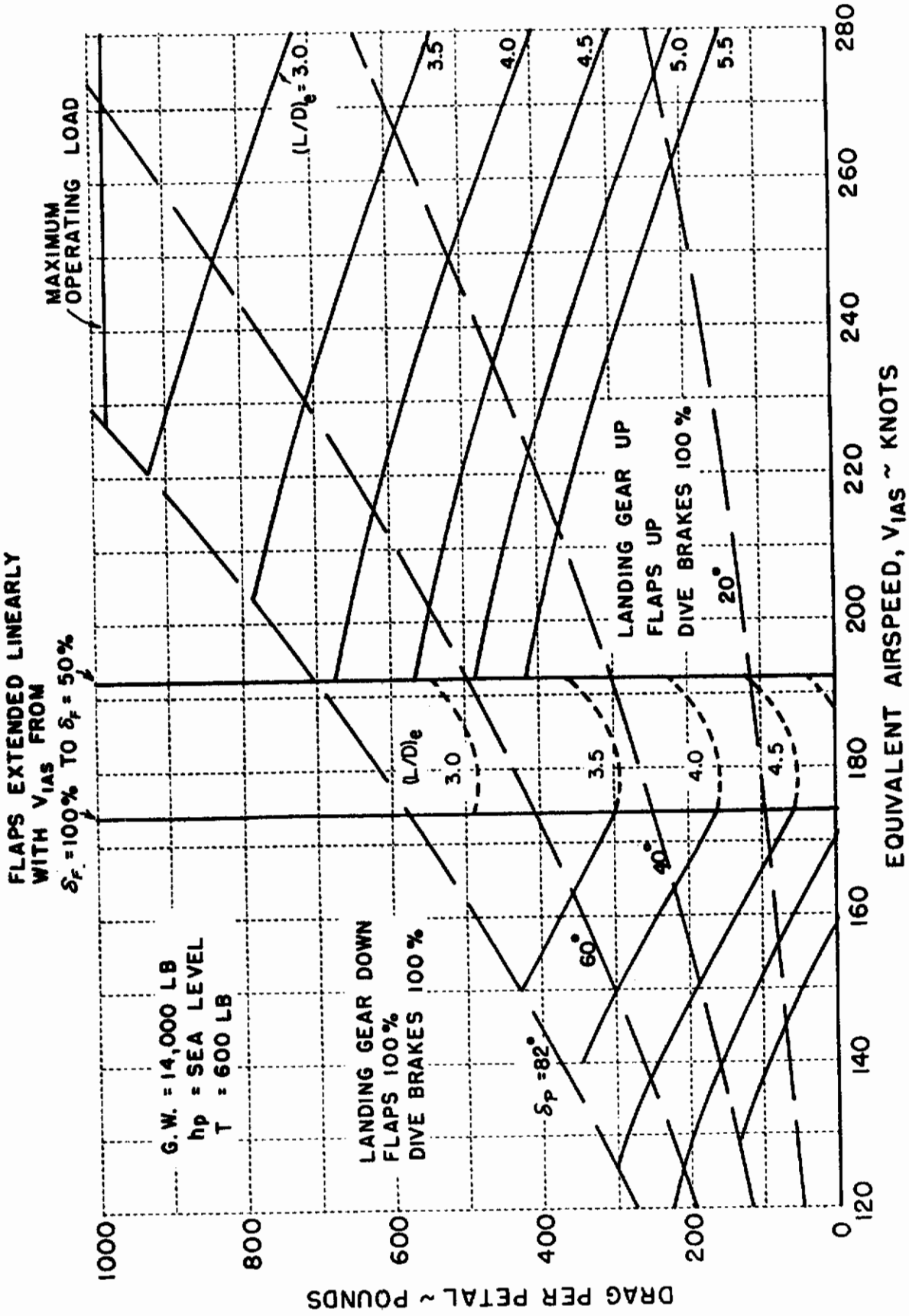

FIGURE 34 SEA LEVEL SUMMARY PLOT

REFERENCES

1. Kelley, M. W.; Greif, R. K.; Tolhurst, W. H., Jr.: Full-Scale Wind Tunnel Tests of a Swept-Wing Airplane With a Cascade-Type Thrust Reverser. NASA TN D-311, April 1960.

2. Tolhurst, W. H., Jr.; Kelley, M. W.; Greif, R. K.: Full-Scale Wind Tunnel Investigation of the Effects of a Target-Type Thrust Reverser on the Low-Speed Aerodynamic Characteristics of a Single-Engine Jet Airplane. NASA TN D-72, September 1959.

3. Anderson, S. B.; Cooper, G. E.; Faye, A. E., Jr.: Flight Measurements of the Effect of a Controllable Thrust Reverser on the Flight Characteristics of a Single-Engine Jet Airplane. NASA Memo 4-26-59A, May 1959.

4. Davies, H. and Kirk, F. N.: A Resumé of Aerodynamic Data on Air Brakes. R & M No. 2614 ARC Technical Report, 1951.

5. Purser, P. E. and Turner, T. R.: Wind-Tunnel Investigation of Perforated Split Flaps for Use as Dive Brakes on a Rectangular NACA 23012 Airfoil. NACA Wartime Report ACR49, July 1941, L-445.

6. Purser, P. E. and Turner, T. E.: Wind-Tunnel Investigation of Perforated Split Flaps for Use as Dive Brakes on a Tapered 23012 Airfoil. NACA Wartime Report ARR93, November 1941, L-373.

7. Hoerner: Fluid Dynamic Drag. Published by the Author.

8. Newell, F. D.: Wind Tunnel Tests of High-Drag Devices on a 10% Scale Model of the T-33 Airplane. CAL Report TE-1462-F-1, December 1960.

9. Newell, F.D.; Rice, R.S., Jr.; Matheis, C.W.; Schelhorn, A.E.: Variable L/D Wind Tunnel Data Analysis and System Design. CAL Report TE-1462-F-2, January 1961.

10. Kinzy, R.F.; Fuller, R.G.; Colman, P.A.; Hong, J.: Air Force Standard Aircraft Characteristics, Performance Substantiation Report for the Lockheed T-33A Airplane. Lockheed Aircraft Corporation, Burbank, California, Report LR 9723, 25 June 1954.

APPENDIX

FUNCTION GENERATOR PROGRAMMING

To aid in programming the nonlinear functions noted on the block diagrams, Figures 15, 16 and 17, charts were prepared and are presented in this appendix. Curves and charts for the nonlinear functions are as follows:

Figure 35	δ_P	feedback calibration
Table 1	$[\delta_{P_1}/\alpha]_{f(V_e)}$	- Basic L/D Profile
Table 2	$[\Delta\alpha/\delta_F]_{f(\delta_F)}$	- Data from Figure 27
Table 3	$[\delta_{P_2}/\delta_F]_{f(\delta_F)}$	- Data from Figure 26
Table 4	$[\delta_e/\delta_F]_{f(\delta_P)}$	- Data from Figure 28
Table 5	$[\delta_e/\delta_P]_{f(\delta_P)}$	- Data from Figure 25

Figure 36 shows the card programming for a linear δ_P/V_e function. The #1 function is for a positive δ_P/V_e motion whereas the #2 function is for negative δ_P/V_e sense. The cockpit gain control for δ_P/V_e is nonlinear, due to potentiometer loading, as shown in Figure 37.

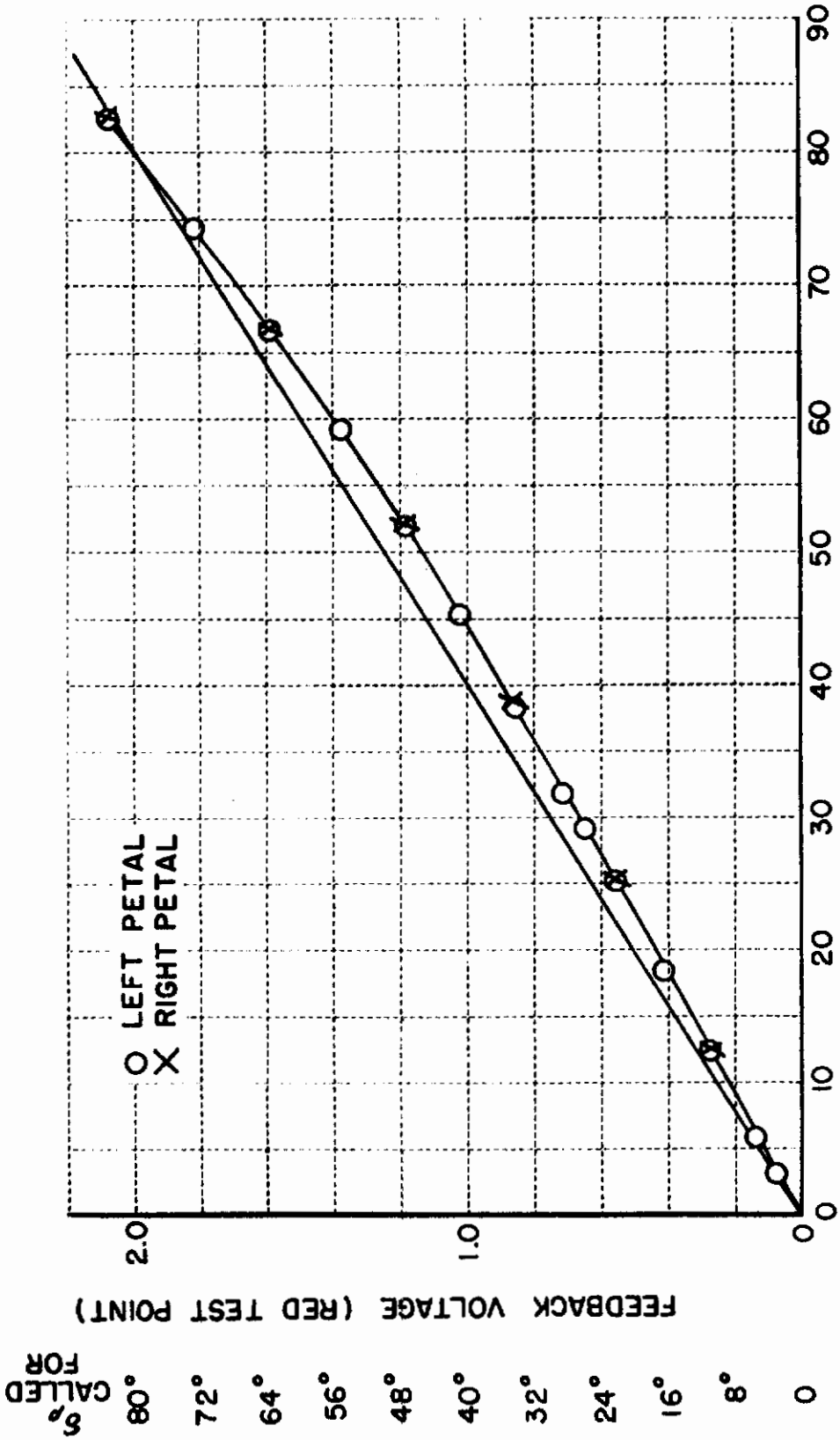

FIGURE 35 FEEDBACK VOLTAGE VS PETAL ANGLE CALIBRATION

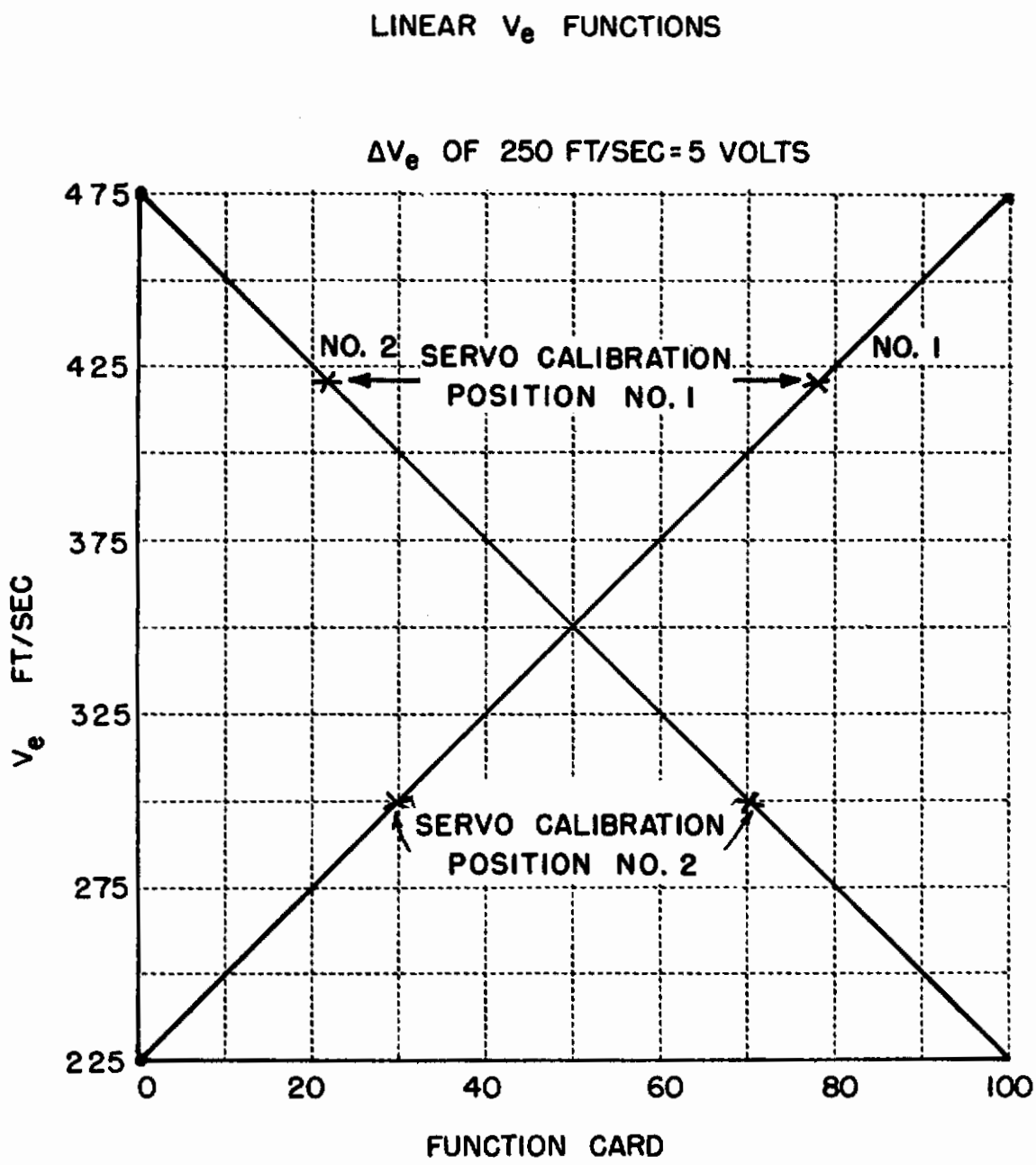

FIGURE 36 LINEAR V_e FUNCTIONS

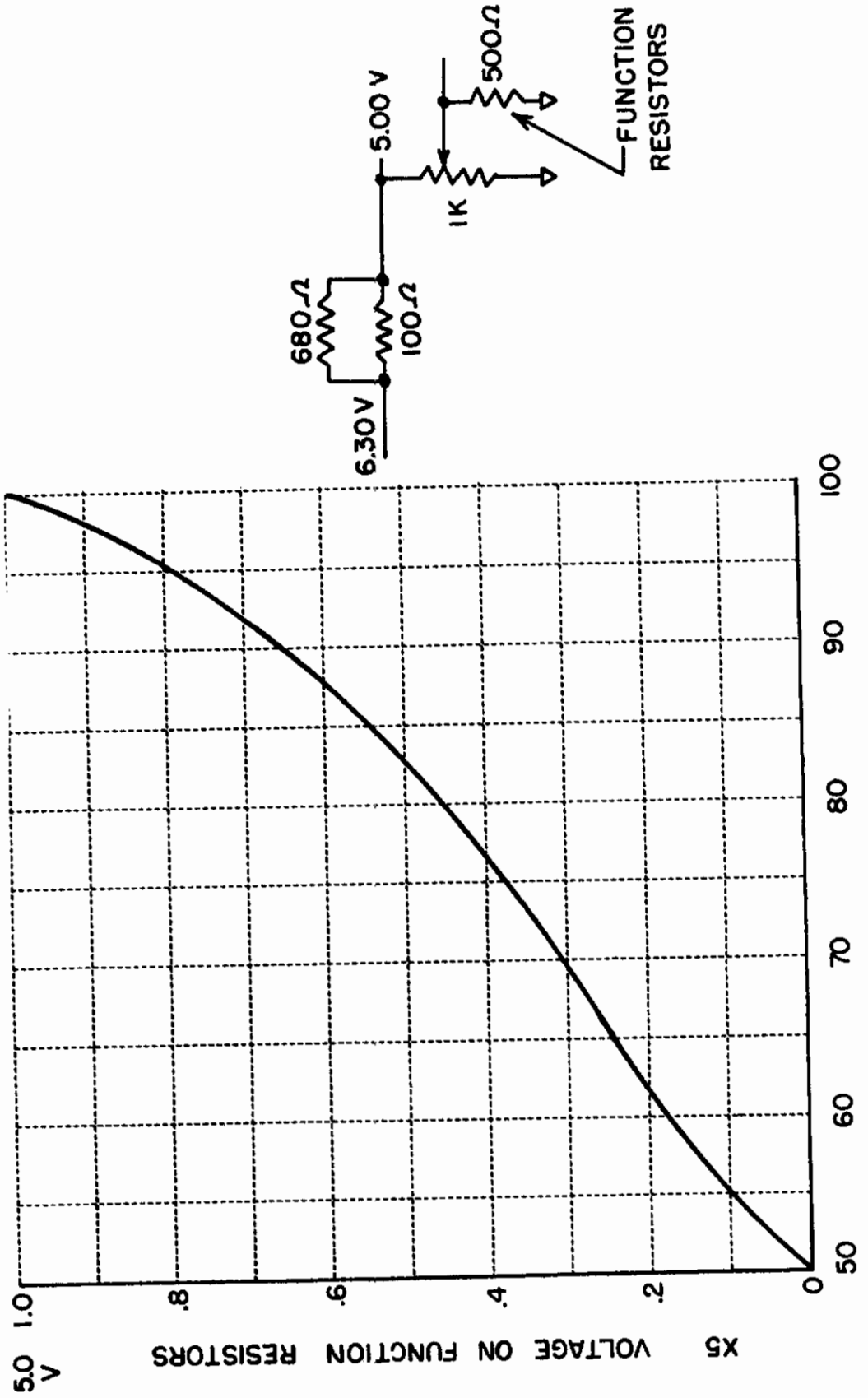

FIGURE 37 NONLINEAR V_e COCKPIT GAIN

TAP	q psi	CALIB. q DIAL	q volts	V_e ft/sec	V_e knots	True α_T deg	CALIB. α_T DIAL	a α_T volts	δ_p deg desired	b δ_p volts	c* card function
-	0	0	0	0	0	∞					
1	.416	3.18	.597	225	133	10.34	103.4	5.17			
2	.475	3.64	.682	240	142	9.06	90.60	4.53			
3	.536	4.11	.761	255	151	8.05	80.50	4.025			
4	.624	4.78	.896	275	162.5	6.94	69.40	3.475			
5	.742	5.68	1.065	300	177.5	5.86	58.60	2.93			
6	.8725	6.69	1.254	325	192	5.00	50.00	2.50			
7	1.01	7.74	1.450	350	207	4.33	43.30	2.165			
8	1.16	8.89	1.665	375	222	3.79	37.90	1.895			
9	1.32	10.1	1.896	400	236.5	3.35	33.50	1.675			
10	1.49	11.4	2.140	425	251.5	2.98	29.80	1.490			
11	1.86	14.25	2.670	475	281	2.42	24.20	1.210			
12	2.49	19.1	3.580	550	325.5	1.84	18.40	0.920			
+	4.04	30.9	5.810	700	414	1.19	11.90	0.595			
Servo Calibration Position											
No. 1			2.02	420	248	3.02	30.20	1.510			
No. 2			1.06	300	177.5	5.86	58.60	2.93			

*c = 2b/a for 200K; c = 4b/a for 400K; c = b/a for 100 K

TABLE 1 L/D PROFILE $\left[\delta_{p_1}/\alpha\right]_{f(V_e)}$

TAP	δ_F deg	δ_F volts	$\Delta\alpha$ deg desired	$\Delta\alpha$ volts 5v = 10°	$\frac{\Delta\alpha}{\delta_F} \sim \frac{\text{volts}}{\text{volt}}$ = Function on Card	200K $\frac{\Delta\alpha}{\delta_F}$	400K $\frac{2\Delta\alpha}{\delta_F}$	100K $\frac{\Delta\alpha}{2\delta_F}$	Function on Card
-									
1	0	0	0	0				65	
2	4.5	.25	.65	.325				65	66
3	9.0	.5	1.32	.66				66	
4	13.5	.75	1.95	.975				65	66
5	18.0	1.00	2.60	1.30				65	
6	22.5	1.25	3.25	1.625				65	66
7	27.0	1.50	3.90	1.95				65	
8	31.5	1.75	4.55	2.28				65	66
9	36.0	2.0	5.15	2.575				64	64
10	40.5	2.25	5.40	2.70				60	60
11	45	2.5	5.50	2.75				55	56

TABLE 2 $\left[\Delta\alpha/\delta_F\right]_{f(\delta_F)}$

TAP	δ_F deg	δ_F volts	δ_{P_2} deg desired	δ_{P_2} volts 5v = 10°	$\frac{\delta_{P_2}}{\delta_F}$ volts/volt Function on Card	200K $\frac{\delta_{P_2}}{\delta_F}$	400K $\frac{2\delta_{P_2}}{\delta_F}$	100K $\frac{\delta_{P_2}}{2\delta_F}$	Function on Card
-									
1	0	0	0	0					44
2	4.5	.25	4.5	.225				45	46
3	9.0	.5	11.0	.55				55.0	56
4	13.5	.75	17.5	.875				58.4	
5	18.0	1.00	23.0	1.15				57.5	58
6	22.5	1.25	28.5	1.43				57.2	
7	27.0	1.50	33.5	1.67				55.6	56
8	31.5	1.75	38.5	1.92				55.0	
9	36.0	2.0	43.0	2.15				53.6	54
10	40.5	2.25	47.5	2.38				52.5	
11	45.	2.5	52.0	2.6				52	52

TABLE 3 $\left[\delta_{P_2}/\delta_F\right]_{f(\delta_F)}$

TAP	δ_F deg	δ_F volts	δ_e deg desired	δ_e volts 1v = 10°	Function on Card Equals 100K $\frac{2\delta_e}{\delta_F}$	200K $\frac{4\delta_e}{\delta_F}$	400K $\frac{8\delta_e}{\delta_F}$	0 = 100 50 = 0	Actual Function on Card	δ_e Check
-										
1	0	0	0	0					16	
2	4.5	.1	.35	.035	70			15		
3	9.0	.2	.72	.072	72			14	14	.72
4	13.5	.3	1.10	.110	73.4			13.3		
5	18.0	.4	1.50	.150	74.8			12.6	12	1.52
6	22.5	.5	1.93	.193	77.4			11.3		
7	27.0	.6	2.40	.240	80			10	10	
8	31.5	.7	2.90	.290	83			8.5	8	2.92
9	36.0	.8	3.48	.348	87.0			6.5	6	3.51
10	40.5	.9	4.15	.415	92.3			3.8	4	4.14
11	45	1.0	5.0	.50	100			0	0	5.0

TABLE 4 $\left[\delta_e/\delta_F\right]_{f(\delta_F)}$

TAP	δ_p Actual	δ_p deg Called For	δ_p volts	δ_e Desired deg lv = 10°	δ_e volts	Function on Card Equals 100K $\frac{2\delta_e}{\delta_p}$	200K $\frac{4\delta_e}{\delta_p}$	400K $\frac{8\delta_e}{\delta_p}$	Function on Card	δ_e Check
1	0	0	0	0	0					
2	9.2	8	.08	+.22	.022	55			7 78	.225
3	18.5	16	.16	+.35	.035	43.8			72	.35
4	27.5	24	.24	+.50	.050	41.6				
5	36.0	32	.32	+.65	.065	40.6			70	.64
6	44.5	40	.40	+.60	.060	30			64	.56
7	52.5	48	.48	+.45	.045	18.8			60	.48
8	60.0	56	.56	+.275	.0275	9.8			56	.336
9	67.0	64	.64	+.10	.010	3.1			52	.128
10	73.5	72	.72	-.04	-.004	1.1			0	0
11	80	80	.8	-.13	-.013	3.25			48	-.16

TABLE 5 $\left[\delta_e/\delta_p\right]_{f(\delta_p)}$